

## FEATURES

**Operating RF and LO frequency: 400 MHz to 6 GHz**

**Input IP3**

30 dBm at 900 MHz

28 dBm at 1900 MHz

**Input IP2: >65 dBm at 900 MHz**

**Input P1dB (IP1dB): 11.6 dBm at 900 MHz**

**Noise figure (NF)**

10.9 dB at 900 MHz

11.7 dB at 1900 MHz

**Voltage conversion gain: ~7 dB**

**Quadrature demodulation accuracy at 900 MHz**

Phase accuracy: ~0.2°

Amplitude balance: ~0.07 dB

**Demodulation bandwidth: ~390 MHz**

**Baseband I/Q drive: 2 V p-p into 200 Ω**

**Single 5 V supply**

## APPLICATIONS

Cellular W-CDMA/GSM/LTE

Microwave point-to-(multi)point radios

Broadband wireless and WiMAX

## GENERAL DESCRIPTION

The **ADL5380** is a broadband quadrature I-Q demodulator that covers an RF/IF input frequency range from 400 MHz to 6 GHz. With a NF = 10.9 dB, IP1dB = 11.6 dBm, and IIP3 = 29.7 dBm at 900 MHz, the **ADL5380** demodulator offers outstanding dynamic range suitable for the demanding infrastructure direct-conversion requirements. The differential RF inputs provide a well-behaved broadband input impedance of 50 Ω and are best driven from a 1:1 balun for optimum performance.

Excellent demodulation accuracy is achieved with amplitude and phase balances of ~0.07 dB and ~0.2°, respectively. The demodulated in-phase (I) and quadrature (Q) differential outputs are fully buffered and provide a voltage conversion gain of ~7 dB. The buffered baseband outputs are capable of driving a 2 V p-p differential signal into 200 Ω.

## FUNCTIONAL BLOCK DIAGRAM

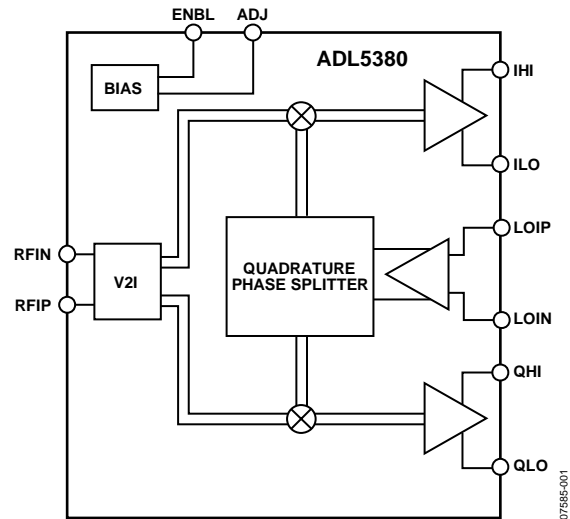


Figure 1.

The fully balanced design minimizes effects from second-order distortion. The leakage from the LO port to the RF port is <math><-50\text{ dBm}</math>. Differential dc offsets at the I and Q outputs are typically <math><20\text{ mV}</math>. Both of these factors contribute to the excellent IIP2 specification, which is >65 dBm.

The **ADL5380** operates off a single 4.75 V to 5.25 V supply. The supply current is adjustable by placing an external resistor from the ADJ pin to either the positive supply,  $V_s$ , (to increase supply current and improve IIP3) or to ground (which decreases supply current at the expense of IIP3).

The **ADL5380** is fabricated using the Analog Devices, Inc., advanced silicon-germanium bipolar process and is available in a 24-lead exposed paddle LFCSP.

Rev. B

[Document Feedback](#)

Information furnished by Analog Devices is believed to be accurate and reliable. However, no responsibility is assumed by Analog Devices for its use, nor for any infringements of patents or other rights of third parties that may result from its use. Specifications subject to change without notice. No license is granted by implication or otherwise under any patent or patent rights of Analog Devices. Trademarks and registered trademarks are the property of their respective owners.

## TABLE OF CONTENTS

Features .....	1	LO Interface .....	22
Applications .....	1	V-to-I Converter .....	22
Functional Block Diagram .....	1	Mixers .....	22
General Description .....	1	Emitter Follower Buffers .....	22
Revision History .....	2	Bias Circuit .....	22
Specifications .....	3	Applications Information .....	23
Absolute Maximum Ratings .....	5	Basic Connections .....	23
ESD Caution .....	5	Power Supply .....	23
Pin Configuration and Function Descriptions .....	6	Local Oscillator and RF Inputs .....	24
Typical Performance Characteristics .....	7	Baseband Outputs .....	25
Low Band Operation .....	7	Error Vector Magnitude (EVM) Performance .....	25
Midband Operation .....	11	Low IF Image Rejection .....	26
High Band Operation .....	14	Example Baseband Interface .....	27
Distributions for $f_{LO} = 900$ MHz .....	17	Characterization Setups .....	31
Distributions for $f_{LO} = 1900$ MHz .....	18	Evaluation Board .....	33
Distributions for $f_{LO} = 2700$ MHz .....	19	Thermal Grounding and Evaluation Board Layout .....	35
Distributions for $f_{LO} = 3600$ MHz .....	20	Outline Dimensions .....	36
Distributions for $f_{LO} = 5800$ MHz .....	21	Ordering Guide .....	36
Circuit Description .....	22		

## REVISION HISTORY

### 12/14—Rev. A to Rev. B

Changes to Figure 2 and Table 3 .....	6
Updated Outline Dimensions .....	36
Changes to Ordering Guide .....	36

### 7/13—Rev. 0 to Rev. A

Changes to Table 2 .....	5
Deleted Local Oscillator (LO) Input Section .....	23
Changed RF Input Section to Local Oscillator and RF Inputs Section .....	24
Added Figure 78, Figure 79, and Figure 82, Renumbered Sequentially .....	24
Added Figure 83 and Figure 84 .....	25
Changes to Evaluation Board Section and Figure 102 .....	33
Changes to Table 5 and Figure 103 Caption .....	34
Deleted Figure 100, Figure 101, and Figure 102 .....	34
Updated Outline Dimensions .....	36
Changes to Ordering Guide .....	36

### 7/09—Revision 0: Initial Version

## SPECIFICATIONS

$V_S = 5\text{ V}$ ,  $T_A = 25^\circ\text{C}$ ,  $f_{LO} = 900\text{ MHz}$ ,  $f_{IF} = 4.5\text{ MHz}$ ,  $P_{LO} = 0\text{ dBm}$ ,  $Z_O = 50\ \Omega$ , unless otherwise noted. Baseband outputs differentially loaded with  $450\ \Omega$ . Loss of the balun used to drive the RF port was de-embedded from these measurements.

Table 1.

Parameter	Condition	Min	Typ	Max	Unit
OPERATING CONDITIONS					
LO and RF Frequency Range		0.4		6	GHz
LO INPUT					
Input Return Loss	LOIP, LOIN		-10		dB
LO Input Level	LO driven differentially through a balun at 900 MHz	-6	0	+6	dBm
I/Q BASEBAND OUTPUTS					
Voltage Conversion Gain	QHI, QLO, IHI, ILO		6.9		dB
	450 $\Omega$ differential load on I and Q outputs at 900 MHz		5.9		dB
	200 $\Omega$ differential load on I and Q outputs at 900 MHz		390		MHz
Demodulation Bandwidth	1 V p-p signal, 3 dB bandwidth		0.2		Degrees
Quadrature Phase Error	At 900 MHz		0.07		dB
I/Q Amplitude Imbalance			$\pm 10$		mV
Output DC Offset (Differential)	0 dBm LO input at 900 MHz				
Output Common Mode	Dependent on ADJ pin setting				
	$V_{ADJ} \sim 4\text{ V}$ (set by 1.5 k $\Omega$ from ADJ pin to $V_S$ )		$V_S - 2.5$		V
	$V_{ADJ} \sim 4.8\text{ V}$ (set by 200 $\Omega$ from ADJ pin to $V_S$ )		$V_S - 2.8$		V
	$V_{ADJ} \sim 2.4\text{ V}$ (ADJ pin open)		$V_S - 1.2$		V
0.1 dB Gain Flatness			37		MHz
Output Swing	Differential 200 $\Omega$ load		2		V p-p
Peak Output Current	Each pin		12		mA
POWER SUPPLIES					
Voltage	$V_S = VCC1, VCC2, VCC3$	4.75		5.25	V
Current	1.5 k $\Omega$ from ADJ pin to $V_S$ ; ENBL pin low		245		mA
	1.5 k $\Omega$ from ADJ pin to $V_S$ ; ENBL pin high		145		mA
ENABLE FUNCTION					
Off Isolation	Pin ENBL		-70		dB
Turn-On Settling Time	ENBL high to low		45		ns
Turn-Off Settling Time	ENBL low to high		950		ns
ENBL High Level (Logic 1)		2.5			V
ENBL Low Level (Logic 0)				1.7	V
DYNAMIC PERFORMANCE at RF = 900 MHz					
Conversion Gain	$V_{ADJ} \sim 4\text{ V}$ (set by 1.5 k $\Omega$ from ADJ pin to $V_S$ )		6.9		dB
Input P1dB			11.6		dBm
RF Input Return Loss	RFIP, RFIN driven differentially through a balun		-19		dB
Second-Order Input Intercept (IIP2)	-5 dBm each input tone		68		dBm
Third-Order Input Intercept (IIP3)	-5 dBm each input tone		29.7		dBm
LO to RF	RFIN, RFIP terminated in 50 $\Omega$		-52		dBm
RF to LO	LOIN, LOIP terminated in 50 $\Omega$		-67		dBc
IQ Magnitude Imbalance			0.07		dB
IQ Phase Imbalance			0.2		Degrees
Noise Figure			10.9		dB
Noise Figure Under Blocking Conditions	With a -5 dBm input interferer 5 MHz away		13.1		dB

Parameter	Condition	Min	Typ	Max	Unit
<b>DYNAMIC PERFORMANCE at RF = 1900 MHz</b>					
	$V_{ADJ} \sim 4\text{ V}$ (set by 1.5 k $\Omega$ from ADJ pin to $V_S$ )				
Conversion Gain			6.8		dB
Input P1dB			11.6		dBm
RF Input Return Loss	RFIP, RFIN driven differentially through a balun		-13		dB
Second-Order Input Intercept (IIP2)	-5 dBm each input tone		61		dBm
Third-Order Input Intercept (IIP3)	-5 dBm each input tone		27.8		dBm
LO to RF	RFIN, RFIP terminated in 50 $\Omega$		-49		dBm
RF to LO	LOIN, LOIP terminated in 50 $\Omega$		-77		dBc
IQ Magnitude Imbalance			0.07		dB
IQ Phase Imbalance			0.25		Degrees
Noise Figure			11.7		dB
Noise Figure Under Blocking Conditions	With a -5 dBm input interferer 5 MHz away		14		dB
<b>DYNAMIC PERFORMANCE at RF = 2700 MHz</b>					
	$V_{ADJ} \sim 4\text{ V}$ (set by 1.5 k $\Omega$ from ADJ pin to $V_S$ )				
Conversion Gain			7.4		dB
Input P1dB			11		dBm
RF Input Return Loss	RFIP, RFIN driven differentially through a balun		-10		dB
Second-Order Input Intercept (IIP2)	-5 dBm each input tone		54		dBm
Third-Order Input Intercept (IIP3)	-5 dBm each input tone		28		dBm
LO to RF	RFIN, RFIP terminated in 50 $\Omega$		-49		dBm
RF to LO	LOIN, LOIP terminated in 50 $\Omega$		-73		dBc
IQ Magnitude Imbalance			0.07		dB
IQ Phase Imbalance			0.5		Degrees
Noise Figure			12.3		dB
<b>DYNAMIC PERFORMANCE at RF = 3600 MHz</b>					
	$V_{ADJ} \sim 4.8\text{ V}$ (set by 200 $\Omega$ from ADJ pin to $V_S$ )				
Conversion Gain			6.3		dB
Input P1dB			9.6		dBm
RF Input Return Loss	RFIP, RFIN driven differentially through a balun		-11		dB
Second-Order Input Intercept (IIP2)	-5 dBm each input tone		48		dBm
Third-Order Input Intercept (IIP3)	-5 dBm each input tone		21		dBm
LO to RF	RFIN, RFIP terminated in 50 $\Omega$		-46		dBm
RF to LO	LOIN, LOIP terminated in 50 $\Omega$		-72		dBc
IQ Magnitude Imbalance			0.14		dB
IQ Phase Imbalance			1.1		Degrees
Noise Figure			14.2		dB
Noise Figure Under Blocking Conditions	With a -5 dBm input interferer 5 MHz away		16.2		dB
<b>DYNAMIC PERFORMANCE at RF = 5800 MHz</b>					
	$V_{ADJ} \sim 2.4\text{ V}$ (ADJ pin left open)				
Conversion Gain			5.8		dB
Input P1dB			8.2		dBm
RF Input Return Loss	RFIP, RFIN driven differentially through a balun		-7.5		dB
Second-Order Input Intercept (IIP2)	-5 dBm each input tone		44		dBm
Third-Order Input Intercept (IIP3)	-5 dBm each input tone		20.6		dBm
LO to RF	RFIN, RFIP terminated in 50 $\Omega$		-47		dBm
RF to LO	LOIN, LOIP terminated in 50 $\Omega$		-62		dBc
IQ Magnitude Imbalance			0.07		dB
IQ Phase Imbalance			-1.25		Degrees
Noise Figure			15.5		dB
Noise Figure Under Blocking Conditions	With a -5 dBm input interferer 5 MHz away		18.9		dB

## ABSOLUTE MAXIMUM RATINGS

Table 2.

Parameter	Rating
Supply Voltage: VCC1, VCC2, VCC3	5.5 V
LO Input Power	13 dBm (re: 50 $\Omega$ )
RF Input Power	15 dBm (re: 50 $\Omega$ )
Internal Maximum Power Dissipation	1370 mW
$\theta_{JA}$ <sup>1</sup>	53°C/W
$\theta_{JC}$	2.5°C/W
Maximum Junction Temperature	150°C
Operating Temperature Range	-40°C to +85°C
Storage Temperature Range	-65°C to +125°C

<sup>1</sup> Per JEDEC standard JESD 51-2. For information on optimizing thermal impedance, see the Thermal Grounding and Evaluation Board Layout section.

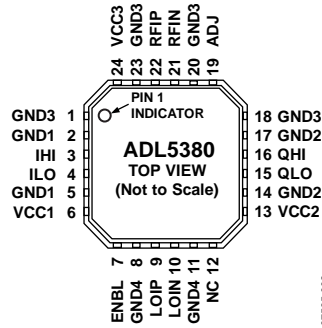
Stresses at or above those listed under Absolute Maximum Ratings may cause permanent damage to the product. This is a stress rating only; functional operation of the product at these or any other conditions above those indicated in the operational section of this specification is not implied. Operation beyond the maximum operating conditions for extended periods may affect product reliability.

### ESD CAUTION



**ESD (electrostatic discharge) sensitive device.** Charged devices and circuit boards can discharge without detection. Although this product features patented or proprietary protection circuitry, damage may occur on devices subjected to high energy ESD. Therefore, proper ESD precautions should be taken to avoid performance degradation or loss of functionality.

## PIN CONFIGURATION AND FUNCTION DESCRIPTIONS



## NOTES

1. NC = NO CONNECT. DO NOT CONNECT TO THIS PIN.
2. THE EXPOSED PAD SHOULD BE CONNECTED TO A LOW IMPEDANCE THERMAL AND ELECTRICAL GROUND PLANE.

Figure 2. Pin Configuration

Table 3. Pin Function Descriptions

Pin No.	Mnemonic	Description
1, 2, 5, 8, 11, 14, 17, 18, 20, 23	GND1, GND2, GND3, GND4	Ground Connect.
3, 4, 15, 16	IHI, ILO, QLO, QHI	I Channel and Q Channel Mixer Baseband Outputs. These outputs have a 50 $\Omega$ differential output impedance (25 $\Omega$ per pin). Each output pair can swing 2 V p-p (differential) into a load of 200 $\Omega$ . The output 3 dB bandwidth is ~400 MHz.
6, 13, 24	VCC1, VCC2, VCC3	Supply. Positive supply for LO, IF, biasing, and baseband sections. Decouple these pins to the board ground using the appropriate-sized capacitors.
7	ENBL	Enable Control. When pulled low, the part is fully enabled; when pulled high, the part is partially powered down and the output is disabled.
9, 10	LOIP, LOIN	Local Oscillator Input. Pins must be ac-coupled. A differential drive through a balun is necessary to achieve optimal performance. Recommended balun is the Mini-Circuits® TC1-1-13 for lower frequencies, the Johanson Technology 3600 balun for midband frequencies, and the Johanson Technology 5400 balun for high band frequencies. Balun choice depends on the desired frequency range of operation.
12	NC	No Connect. Do not connect to this pin.
19	ADJ	A resistor to $V_s$ that optimizes third-order intercept. For operation <3 GHz, $R_{ADJ} = 1.5$ k $\Omega$ . For operation from 3 GHz to 4 GHz, $R_{ADJ} = 200$ $\Omega$ . For operation >5 GHz, $R_{ADJ} =$ open. See the Circuit Description section for more details.
21, 22	RFIN, RFIP	RF Input. A single-ended 50 $\Omega$ signal can be applied differentially to the RF inputs through a 1:1 balun. Recommended balun is the Mini-Circuits TC1-1-13 for lower frequencies, the Johanson Technology 3600 balun for midband frequencies, and the Johanson Technology 5400 balun for high band frequencies. Balun choice depends on the desired frequency range of operation.
	EP	Exposed Pad. The exposed pad should be connected to a low impedance thermal and electrical ground plane.

# TYPICAL PERFORMANCE CHARACTERISTICS

$V_S = 5\text{ V}$ ,  $T_A = 25^\circ\text{C}$ , LO drive level = 0 dBm, RF input balun loss is de-embedded, unless otherwise noted.

## LOW BAND OPERATION

RF = 400 MHz to 3 GHz; Mini-Circuits TC1-1-13 balun on LO and RF inputs, 1.5 kΩ from the ADJ pin to  $V_S$ .

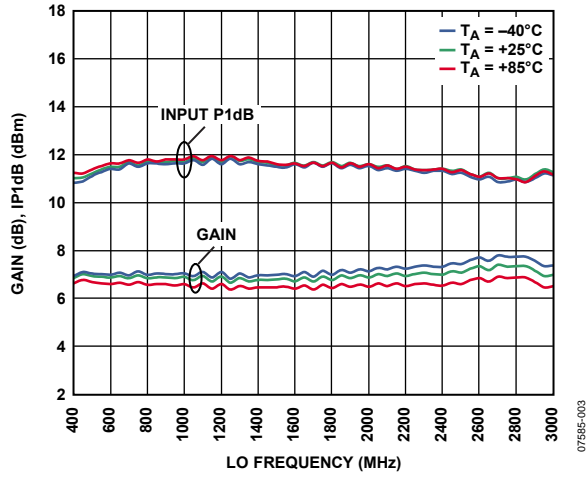


Figure 3. Conversion Gain and Input 1 dB Compression Point (IP1dB) vs. LO Frequency

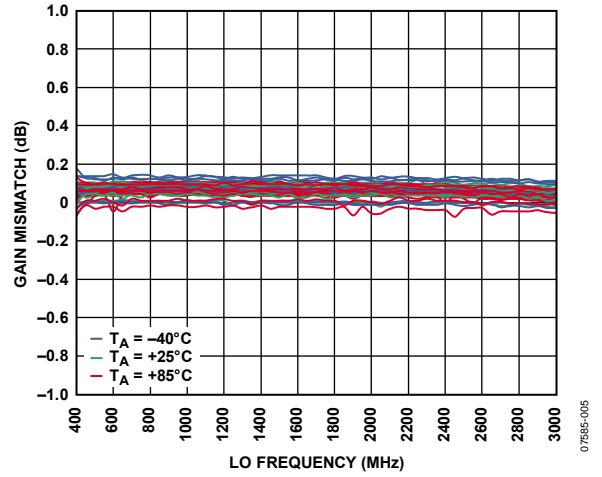


Figure 5. IQ Gain Mismatch vs. LO Frequency

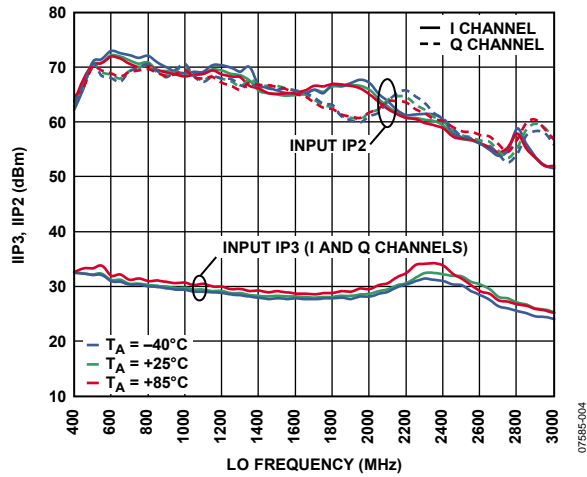


Figure 4. Input Third-Order Intercept (IIP3) and Input Second-Order Intercept Point (IIP2) vs. LO Frequency

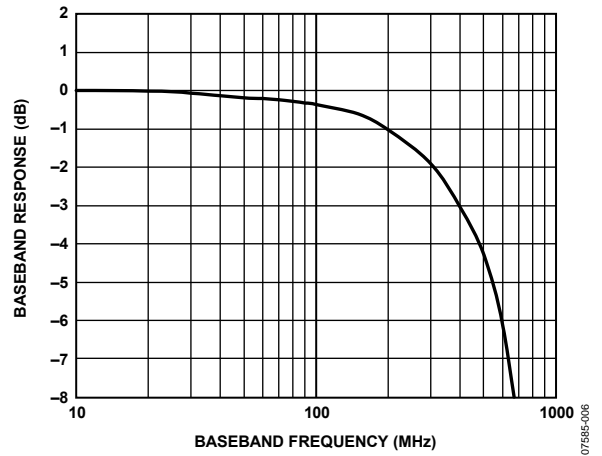


Figure 6. Normalized IQ Baseband Frequency Response

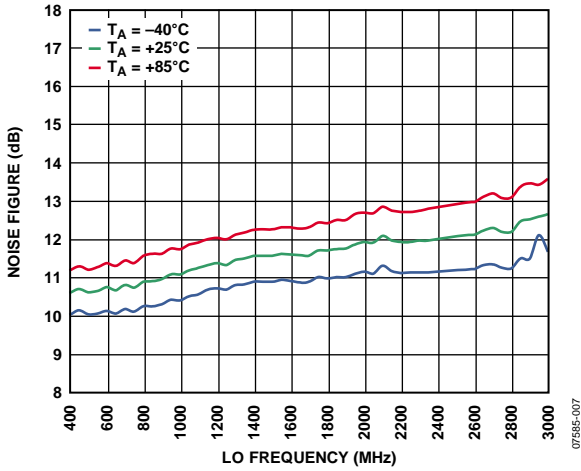


Figure 7. Noise Figure vs. LO Frequency

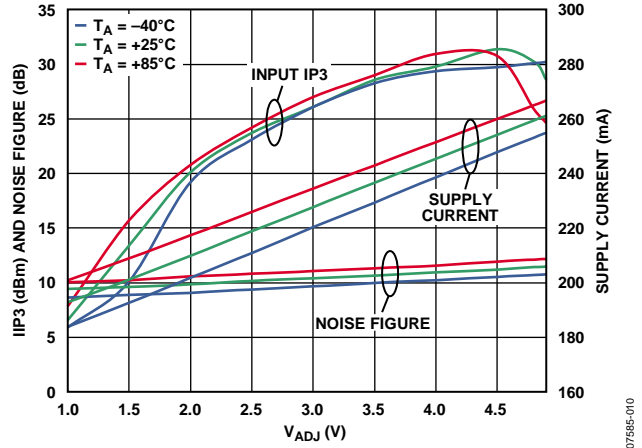


Figure 10. IIP3, Noise Figure, and Supply Current vs.  $V_{ADJ}$ ,  $f_{LO} = 900$  MHz

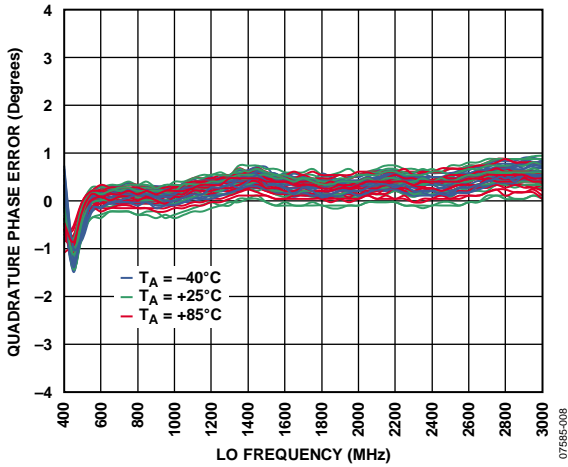


Figure 8. IQ Quadrature Phase Error vs. LO Frequency

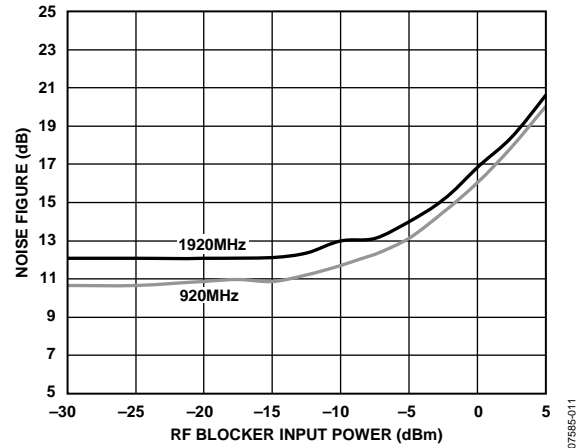


Figure 11. Noise Figure vs. Input Blocker Level,  $f_{LO} = 900$  MHz,  $f_{LO} = 1900$  MHz (RF Blocker 5 MHz Offset)

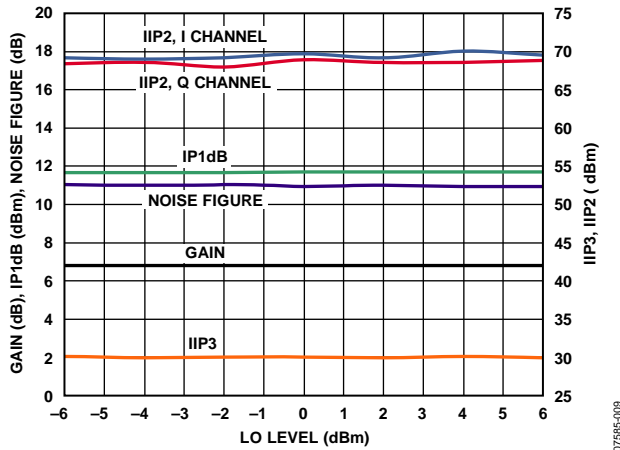


Figure 9. Conversion Gain, IP1dB, Noise Figure, IIP3, and IIP2 vs. LO Level,  $f_{LO} = 900$  MHz

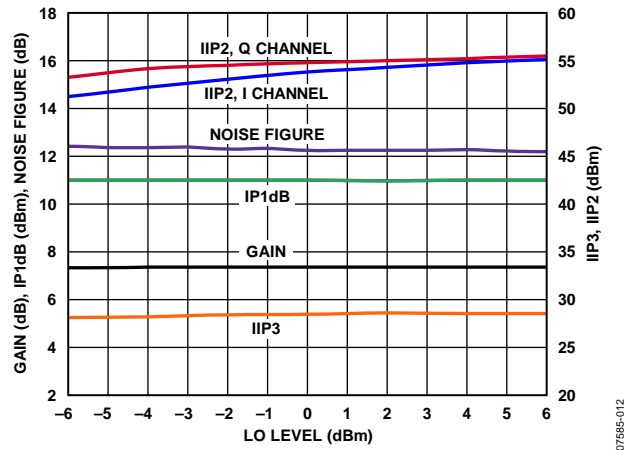


Figure 12. Conversion Gain, IP1dB, Noise Figure, IIP3, and IIP2 vs. LO Level,  $f_{LO} = 2700$  MHz



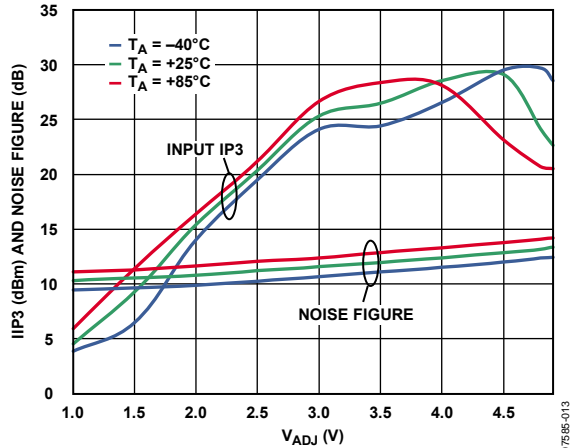


Figure 13. IIP3 and Noise Figure vs.  $V_{ADJ}$ ,  $f_{LO} = 2700$  MHz

07585-013

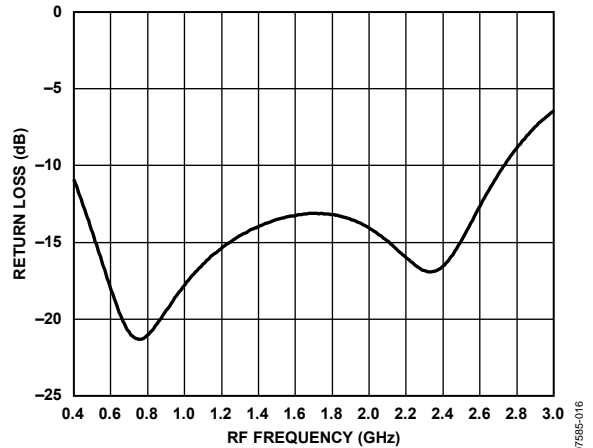


Figure 16. RF Port Return Loss vs. RF Frequency Measured on Characterization Board Through TC1-1-13 Balun

07585-016

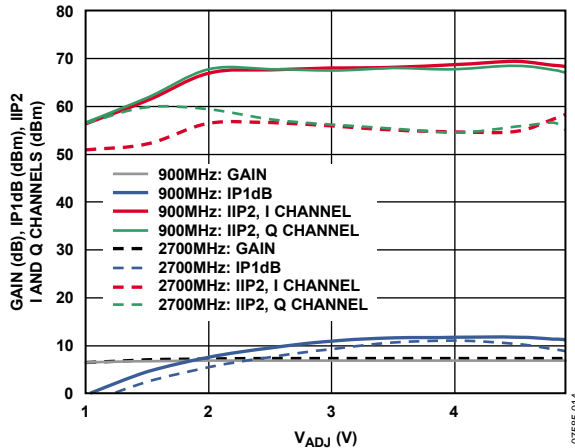


Figure 14. Conversion Gain, IP1dB, and IIP2 vs.  $V_{ADJ}$ ,  $f_{LO} = 900$  MHz,  $f_{LO} = 2700$  MHz

07585-014

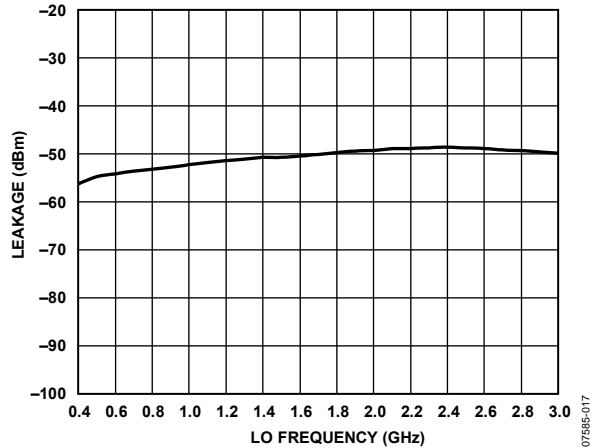


Figure 17. LO-to-RF Leakage vs. LO Frequency

07585-017

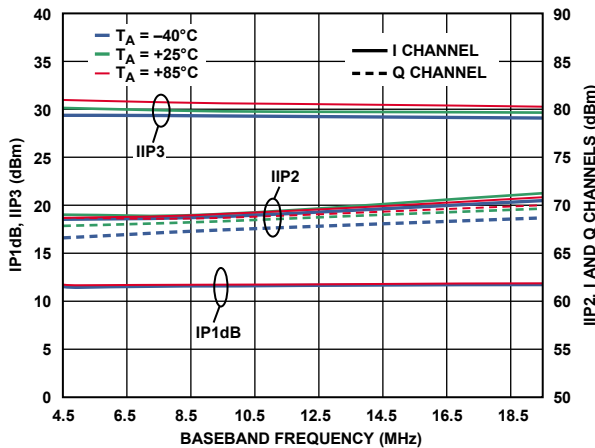


Figure 15. IP1dB, IIP3, and IIP2 vs. Baseband Frequency

07585-015

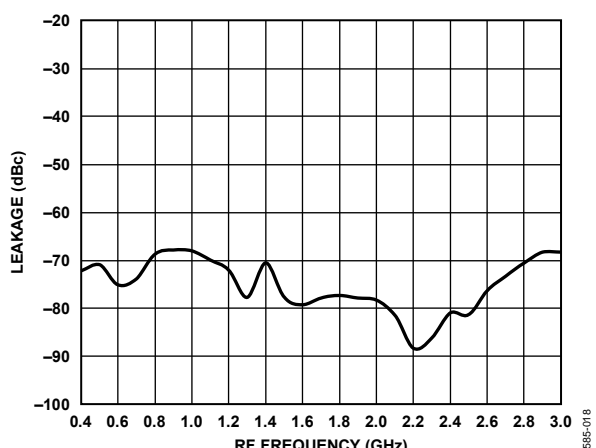


Figure 18. RF-to-LO Leakage vs. RF Frequency

07585-018

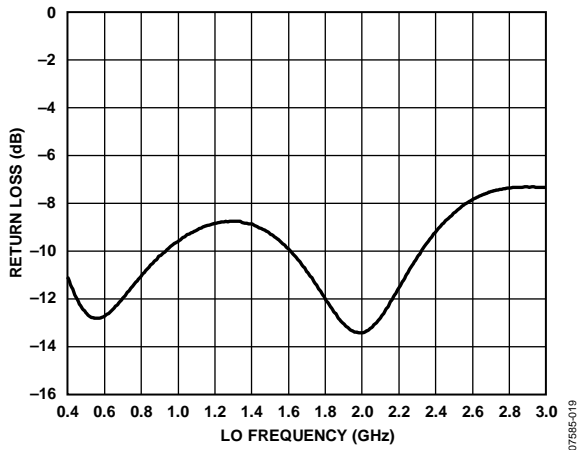


Figure 19. LO Port Return Loss vs. LO Frequency Measured on Characterization Board Through TC1-1-13 Balun

MIDBAND OPERATION

RF = 3 GHz to 4 GHz; Johanson Technology 3600BL14M050T balun on LO and RF inputs, 200 Ω from V<sub>ADJ</sub> to V<sub>S</sub>.

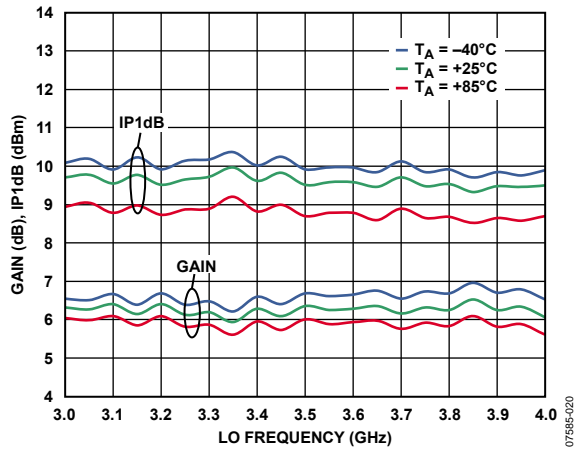


Figure 20. Conversion Gain and Input 1 dB Compression Point (IP1dB) vs. LO Frequency

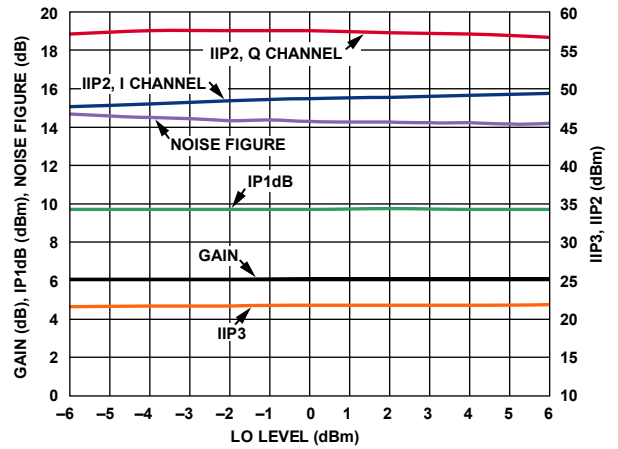


Figure 23. Conversion Gain, IP1dB, Noise Figure, IIP3, and IIP2 vs. LO Level, f<sub>LO</sub> = 3600 MHz

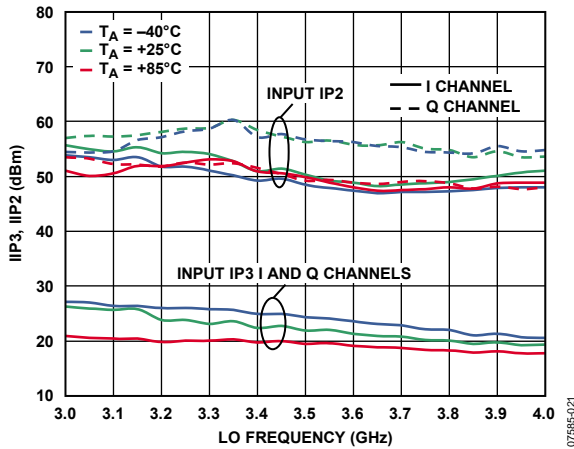


Figure 21. Input Third-Order Intercept (IIP3) and Input Second-Order Intercept Point (IIP2) vs. LO Frequency

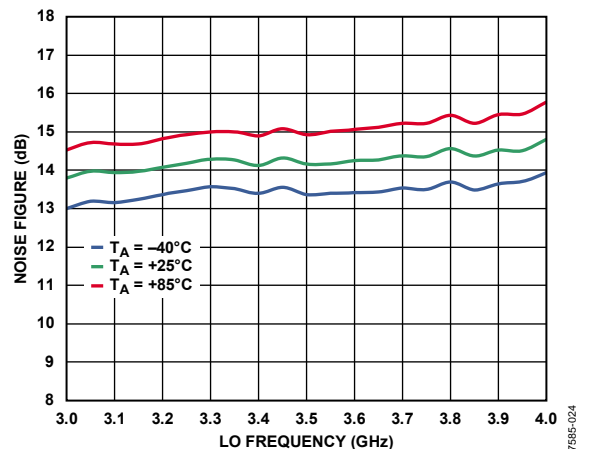


Figure 24. Noise Figure vs. LO Frequency

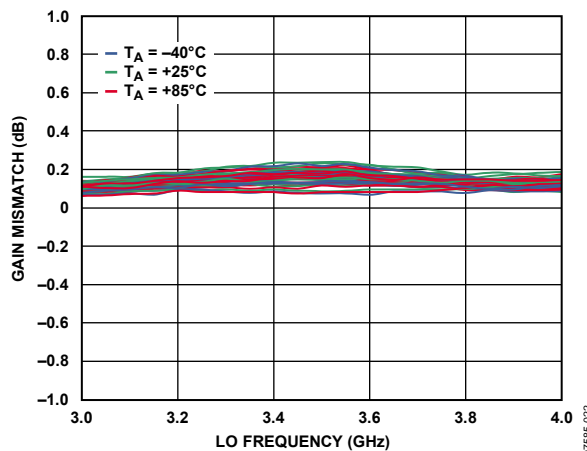


Figure 22. IQ Gain Mismatch vs. LO Frequency

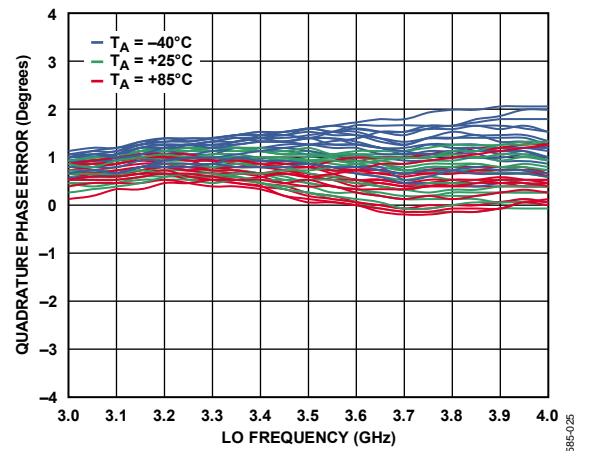
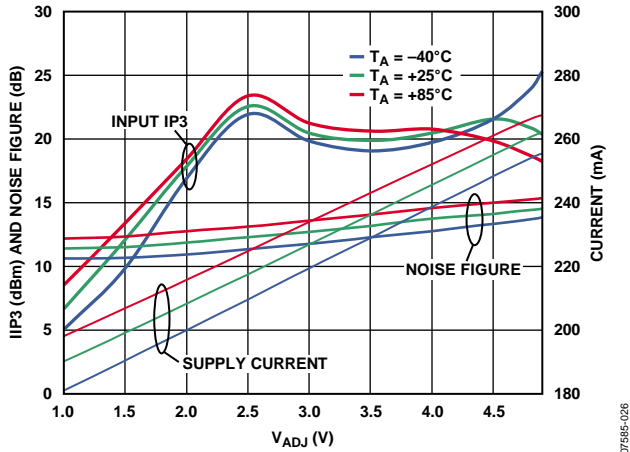
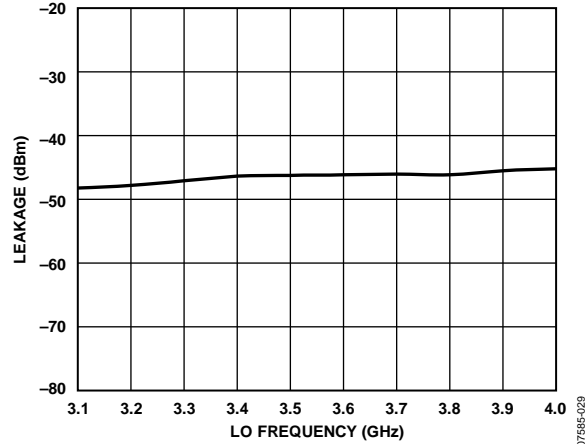


Figure 25. IQ Quadrature Phase Error vs. LO Frequency



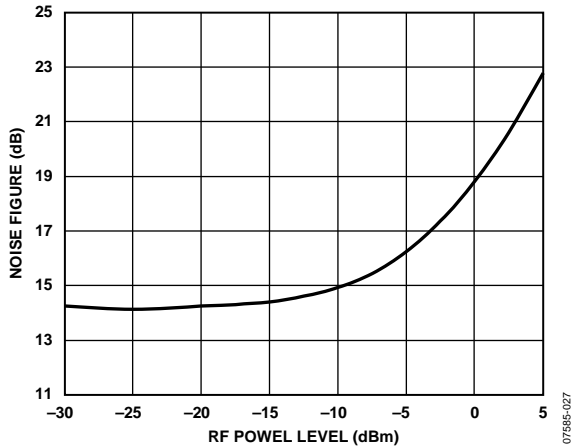
07585-026

Figure 26. IIP3, Noise Figure, and Supply Current vs.  $V_{ADJ}$ ,  $f_{LO} = 3600$  MHz



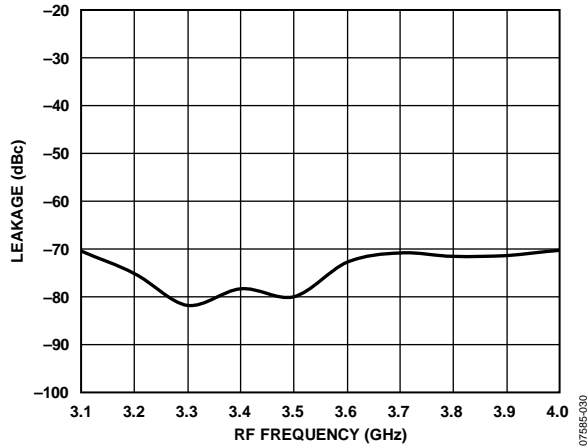
07585-029

Figure 29. LO-to-RF Leakage vs. LO Frequency



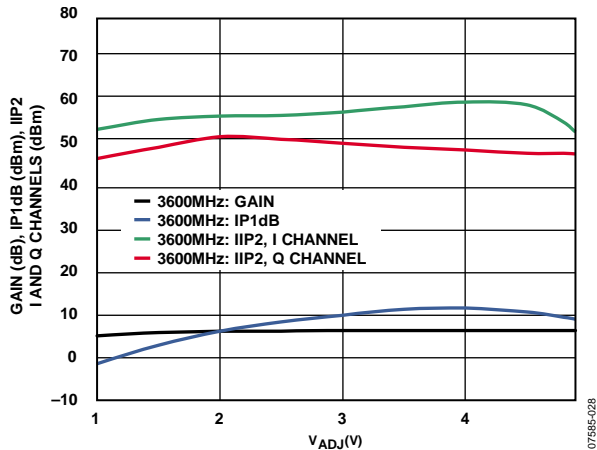
07585-027

Figure 27. Noise Figure vs. Input Blocker Level,  $f_{LO} = 3600$  MHz (RF Blocker 5 MHz Offset)



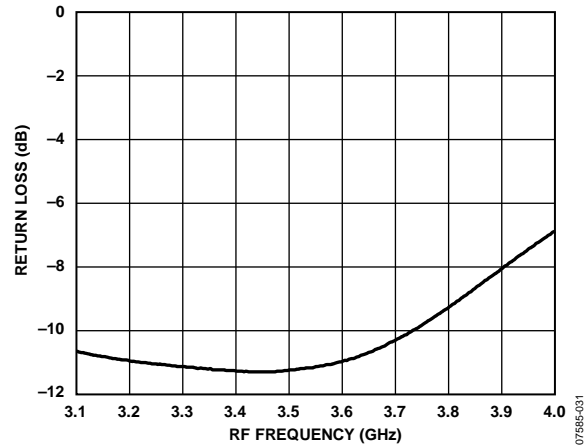
07585-030

Figure 30. RF-to-LO Leakage vs. RF Frequency



07585-028

Figure 28. Conversion Gain, IP1dB, and IIP2 vs.  $V_{ADJ}$ ,  $f_{LO} = 3600$  MHz



07585-031

Figure 31. RF Port Return Loss vs. RF Frequency Measured on Characterization Board Through Johanson Technology 3600 Balun

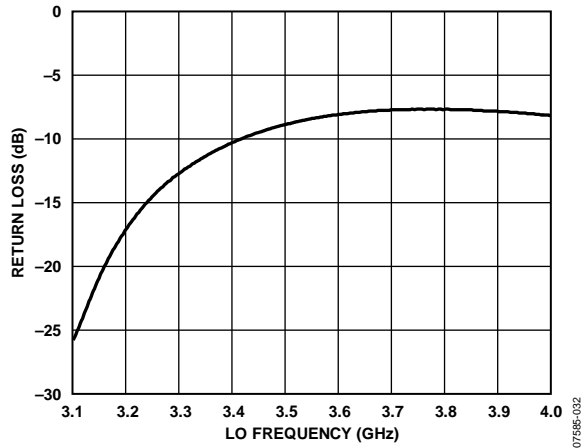


Figure 32. LO Port Return Loss vs. LO Frequency Measured on Characterization Board Through Johanson Technology 3600 Balun

HIGH BAND OPERATION

RF = 5 GHz to 6 GHz; Johanson Technology 5400BL15B050E balun on LO and RF inputs, the ADJ pin is open.

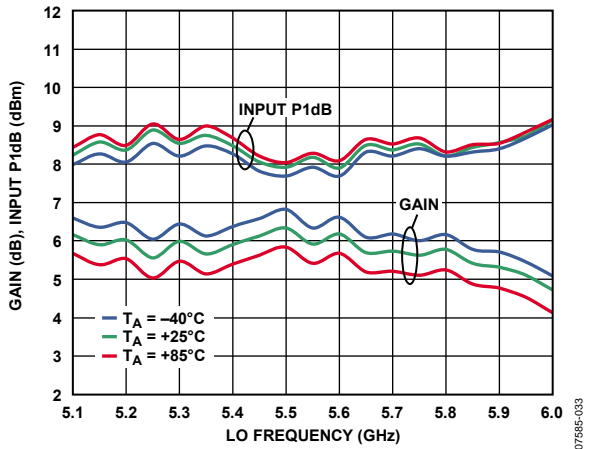


Figure 33. Conversion Gain and Input 1 dB Compression Point (IP1dB) vs. LO Frequency

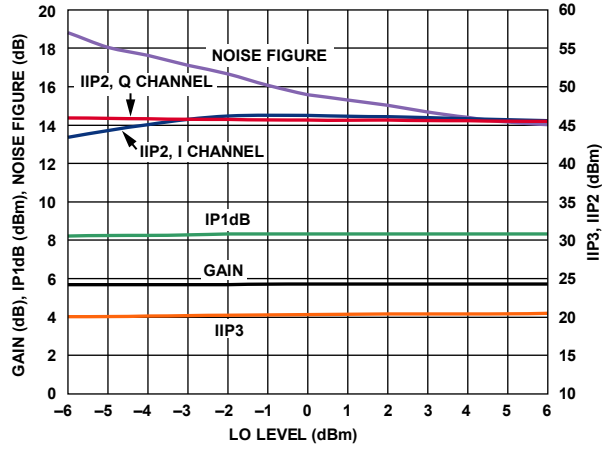


Figure 36. Conversion Gain, IP1dB, Noise Figure, IIP3, and IIP2 vs. LO Level,  $f_{LO} = 5800$  MHz

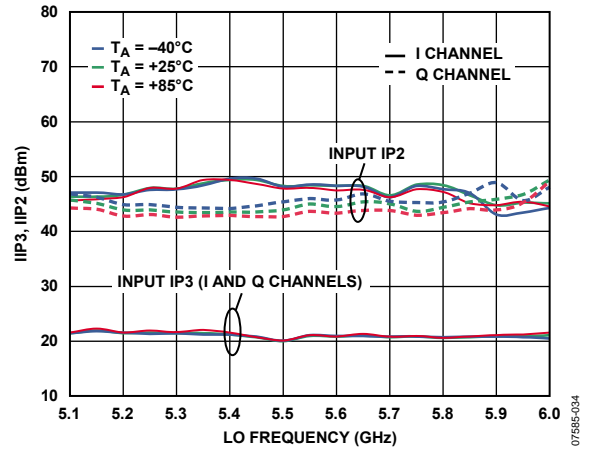


Figure 34. Input Third-Order Intercept (IIP3) and Input Second-Order Intercept Point (IIP2) vs. LO Frequency

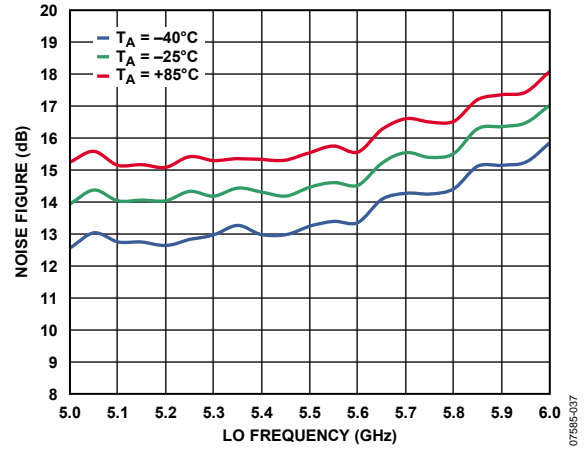


Figure 37. Noise Figure vs. LO Frequency

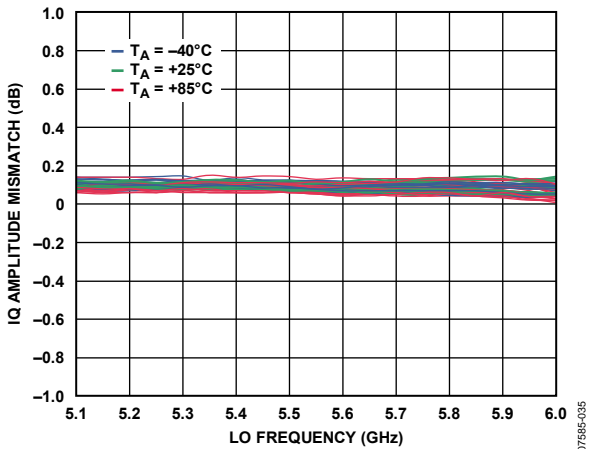


Figure 35. IQ Gain Mismatch vs. LO Frequency

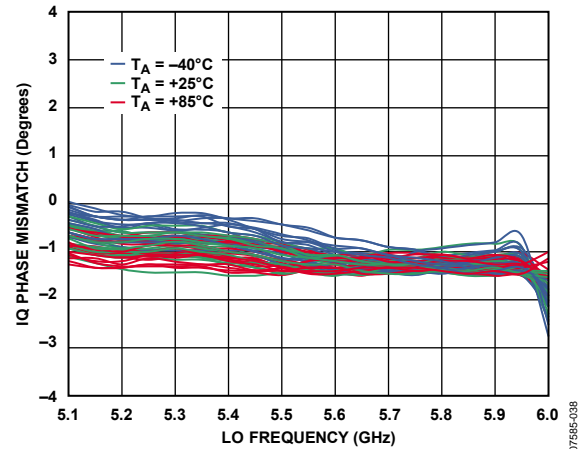


Figure 38. IQ Quadrature Phase Error vs. LO Frequency

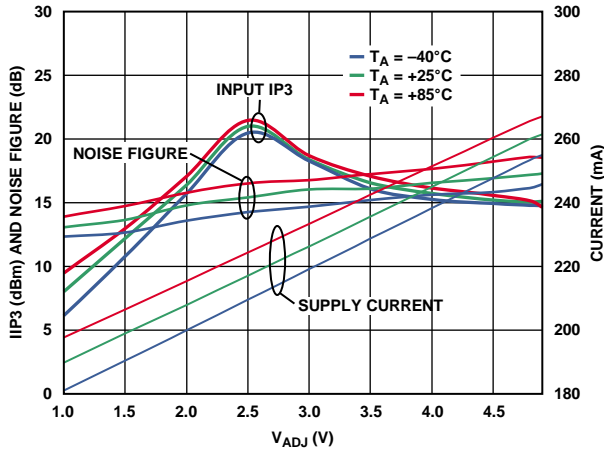


Figure 39. IIP3, Noise Figure, and Supply Current vs.  $V_{ADJ}$ ,  $f_{LO} = 5800$  MHz

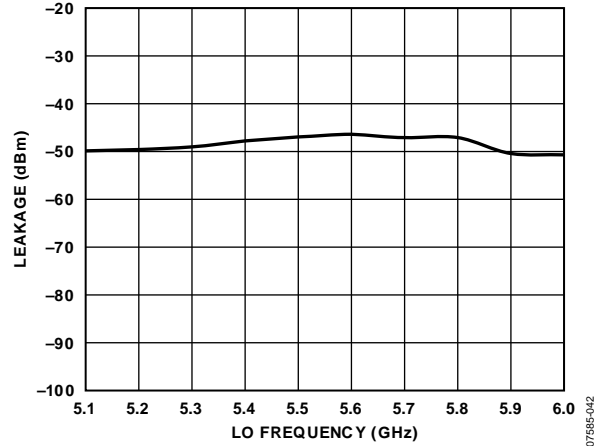


Figure 42. LO-to-RF Leakage vs. LO Frequency

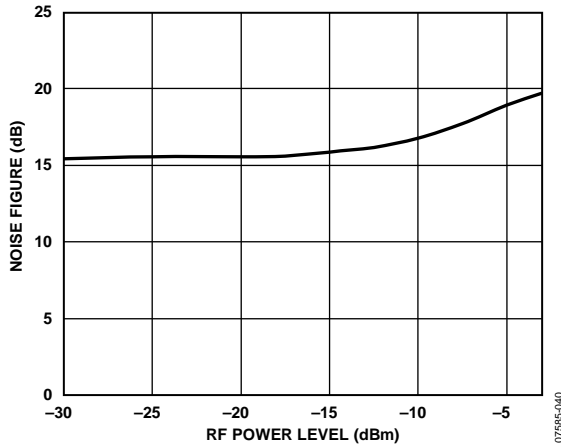


Figure 40. Noise Figure vs. Input Blocker Level,  $f_{LO} = 5800$  MHz (RF Blocker 5 MHz Offset)

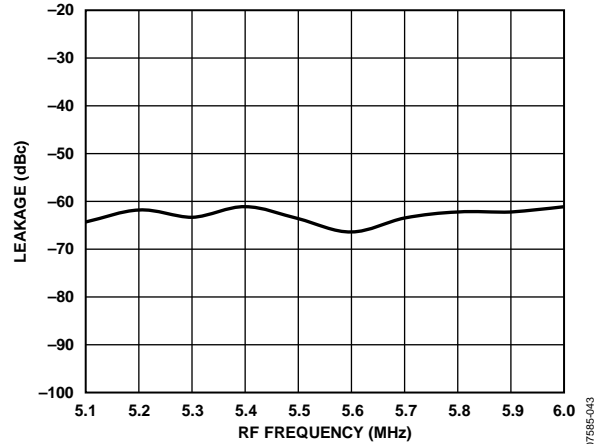


Figure 43. RF-to-LO Leakage vs. RF Frequency

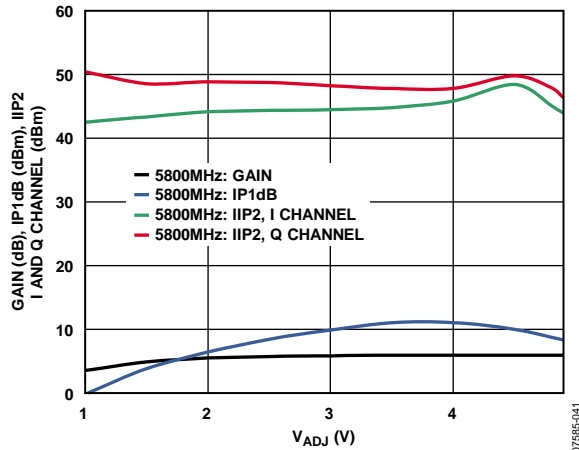


Figure 41. Conversion Gain, IP1dB, and IIP2 vs.  $V_{ADJ}$ ,  $R_{BIAS}$ ,  $f_{LO} = 5800$  MHz

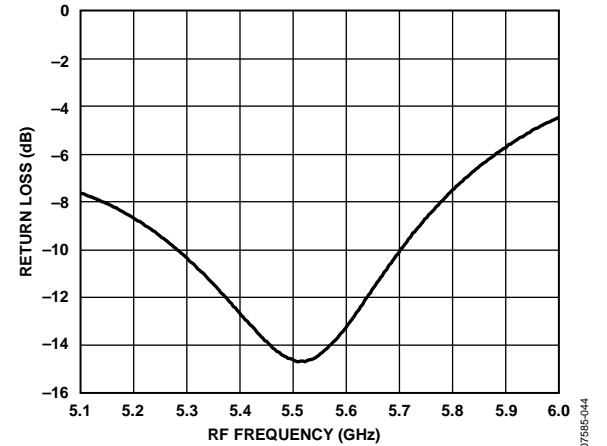


Figure 44. RF Port Return Loss vs. RF Frequency Measured on Characterization Board Through Johanson Technology 5400 Balun

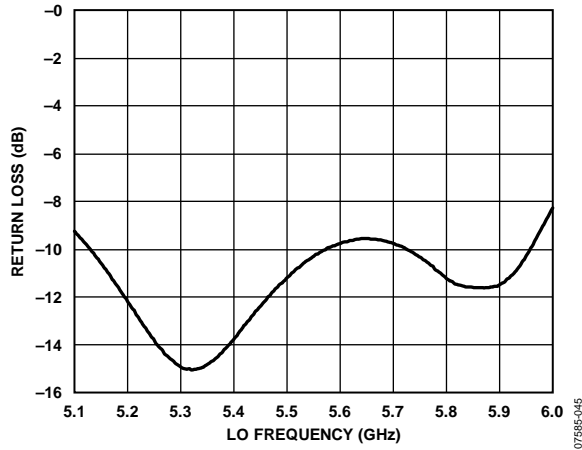


Figure 45. LO Port Return Loss vs. LO Frequency Measured on Characterization Board Through Johanson Technology 5400 Balun



DISTRIBUTIONS FOR  $f_{LO} = 900$  MHz

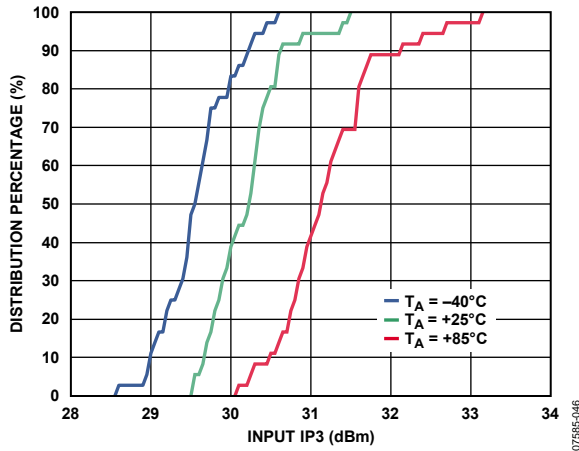


Figure 46. IIP3 Distributions

07585-046

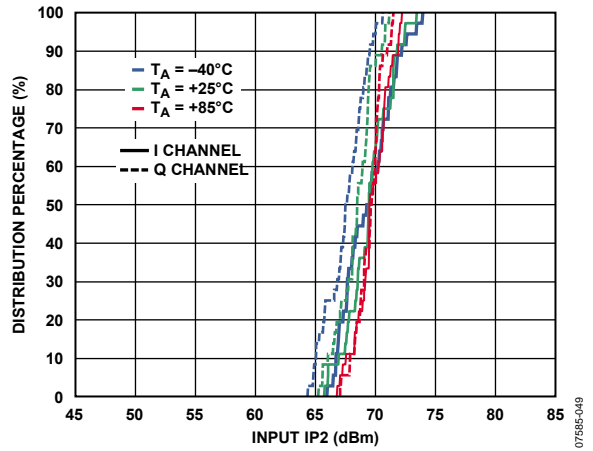


Figure 49. IIP2 Distributions for I Channel and Q Channel

07585-049

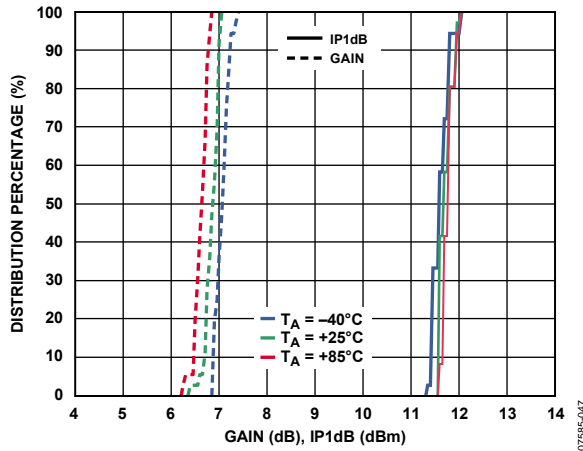


Figure 47. Gain and IP1dB Distributions

07585-047

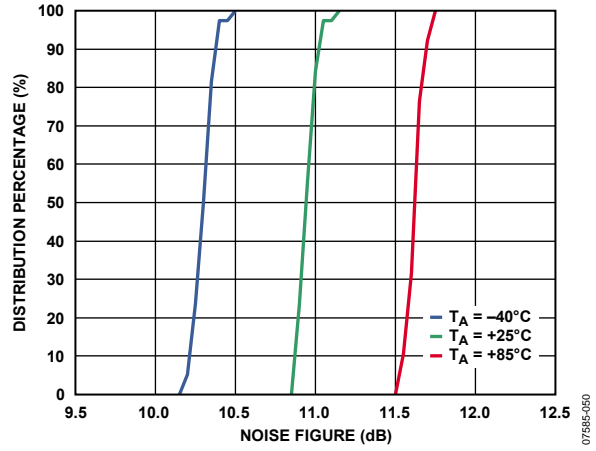


Figure 50. Noise Figure Distributions

07585-050

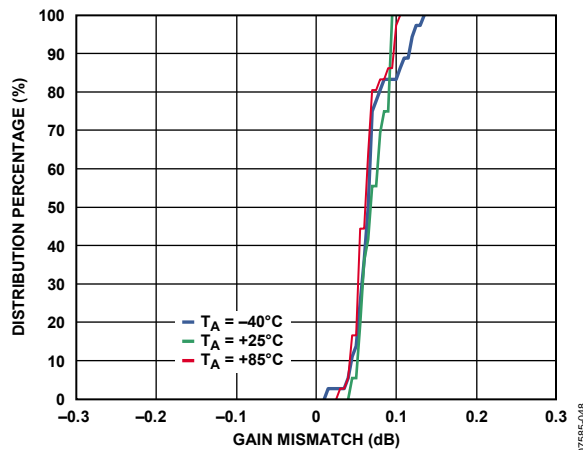


Figure 48. IQ Gain Mismatch Distributions

07585-048

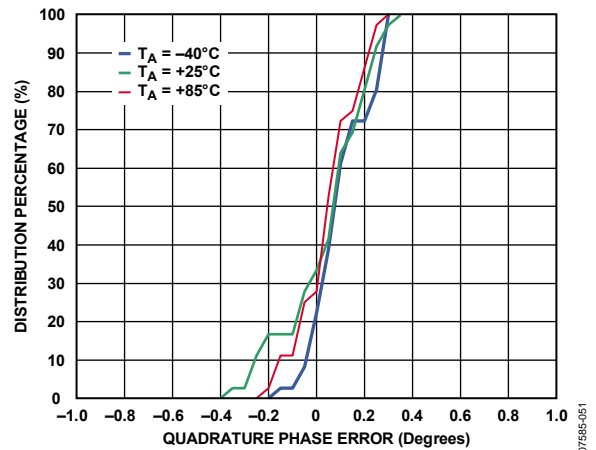


Figure 51. IQ Quadrature Phase Error Distributions

07585-051

DISTRIBUTIONS FOR  $f_{LO} = 1900$  MHz

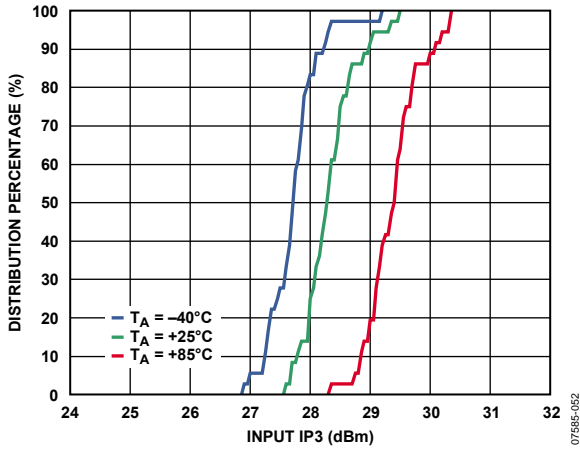


Figure 52. IIP3 Distributions

07595-062

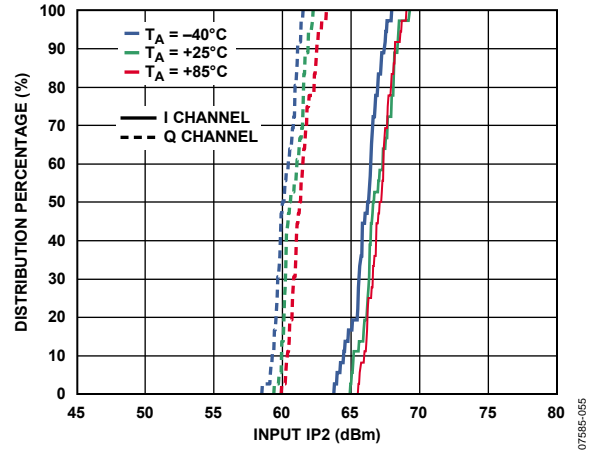


Figure 55. IIP2 Distributions for I Channel and Q Channel

07595-065

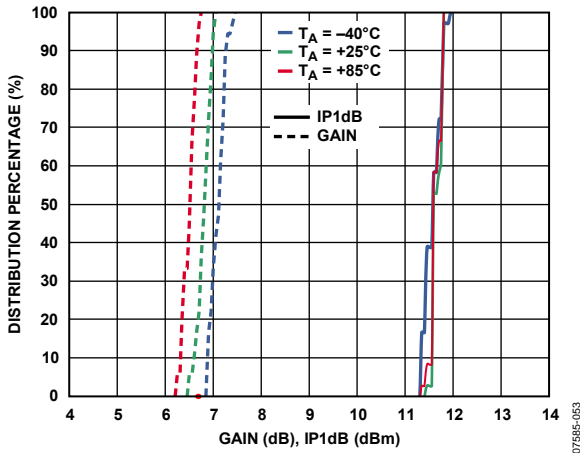


Figure 53. Gain and IP1dB Distributions

07595-063

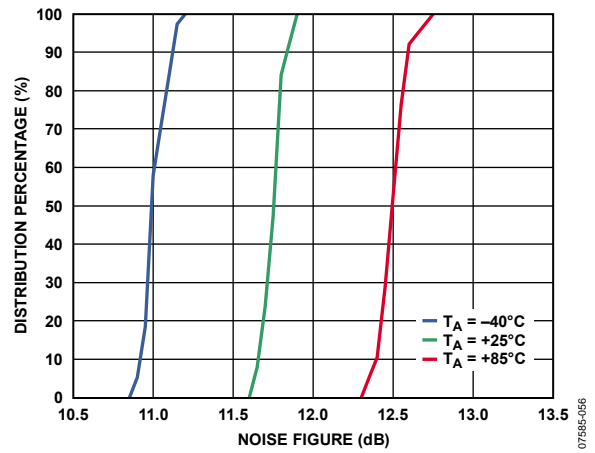


Figure 56. Noise Figure Distributions

07595-066

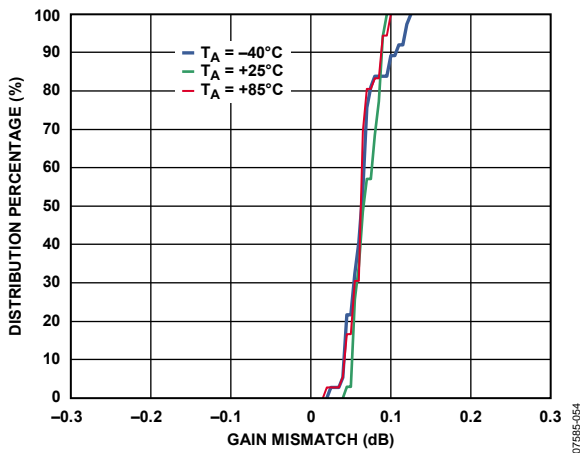


Figure 54. IQ Gain Mismatch Distributions

07595-064

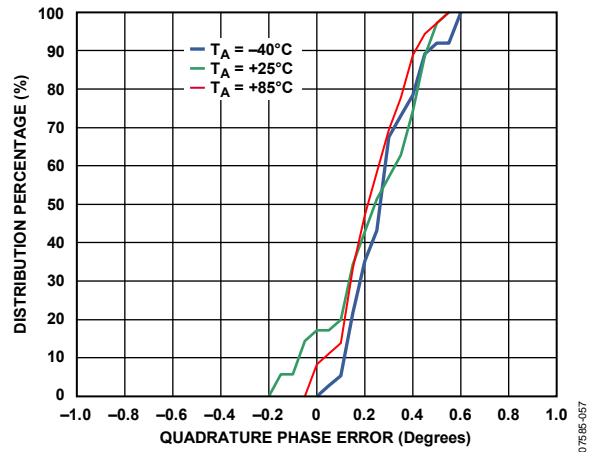


Figure 57. IQ Quadrature Phase Error Distributions

07595-067

DISTRIBUTIONS FOR  $f_{LO} = 2700$  MHz

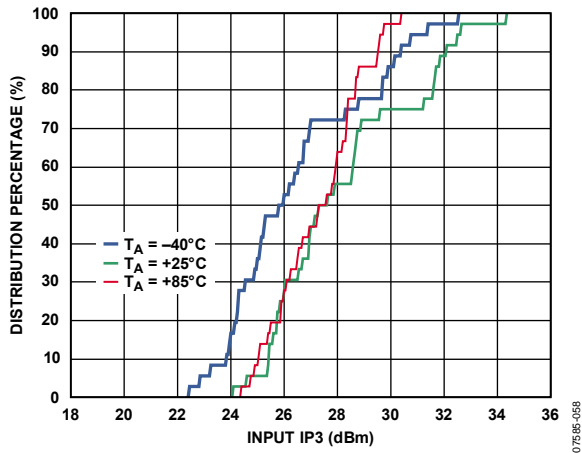


Figure 58. IIP3 Distributions

07595-058

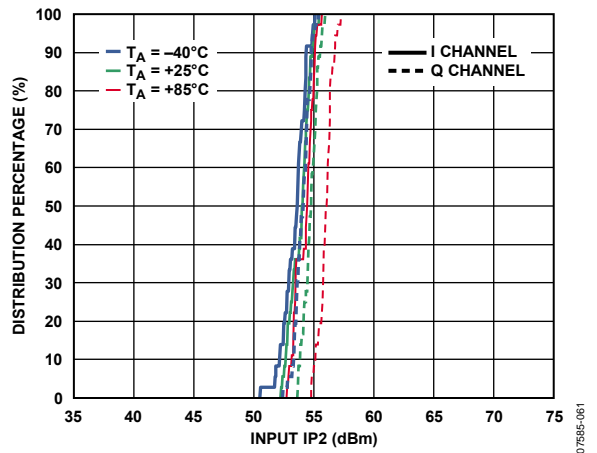


Figure 61. IIP2 Distributions for I Channel and Q Channel

07595-061

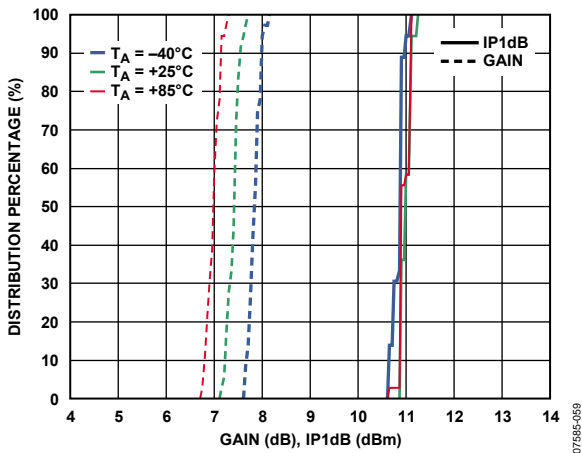


Figure 59. Gain and IP1dB Distributions

07595-059

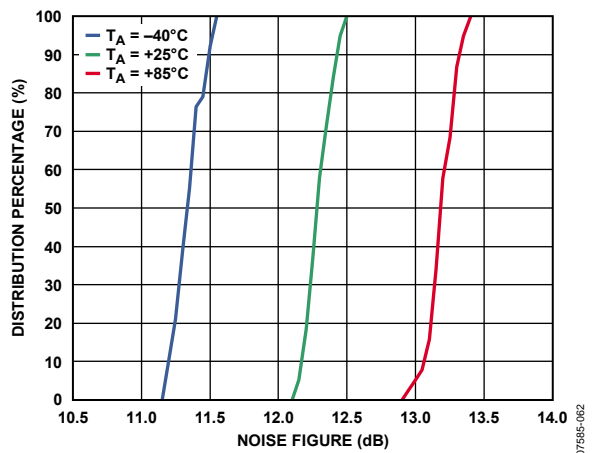


Figure 62. Noise Figure Distributions

07595-062

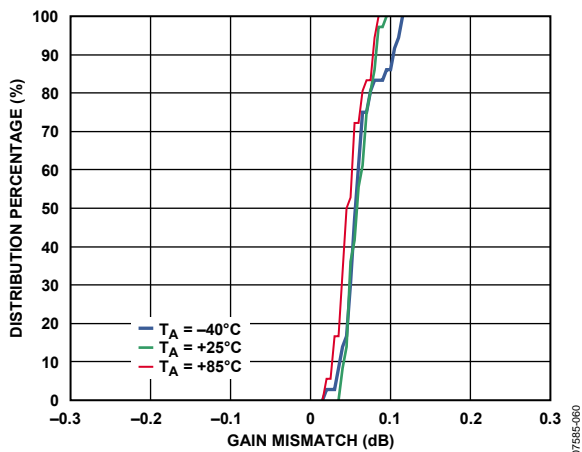


Figure 60. IQ Gain Mismatch Distributions

07595-060

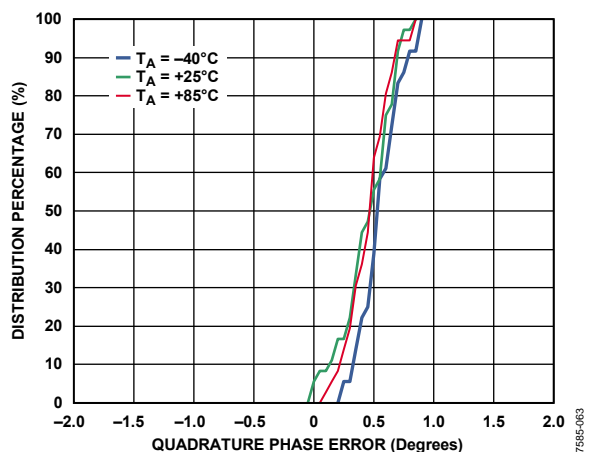


Figure 63. IQ Quadrature Phase Error Distributions

07595-063

DISTRIBUTIONS FOR  $f_{LO} = 3600$  MHz

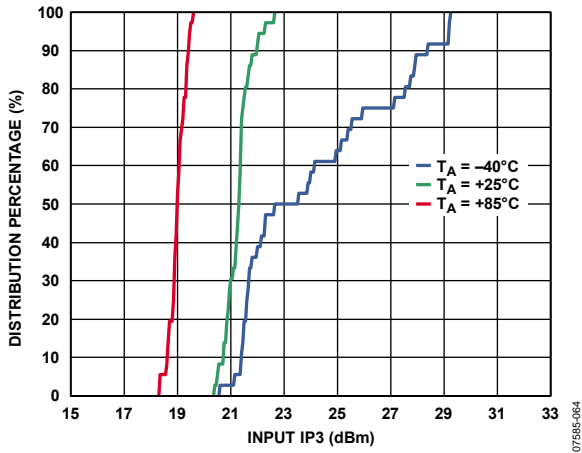


Figure 64. IIP3 Distributions

07595-064

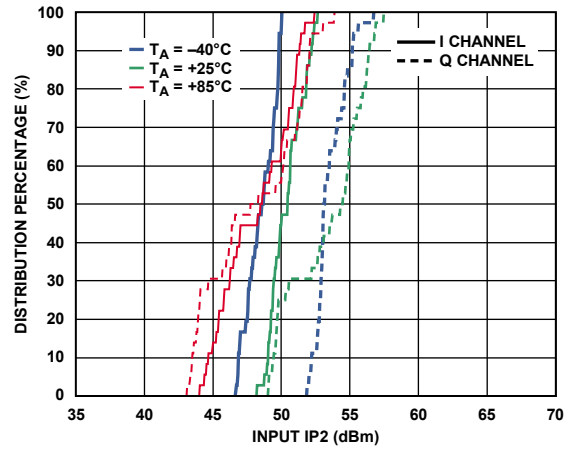


Figure 67. IIP2 Distributions for I Channel and Q Channel

07595-067

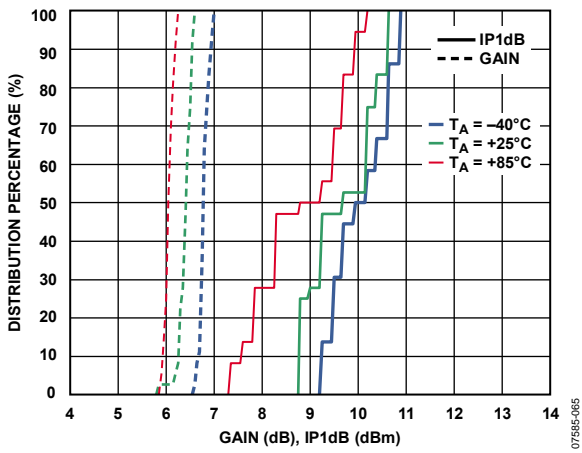


Figure 65. Gain and IP1dB Distributions

07595-065

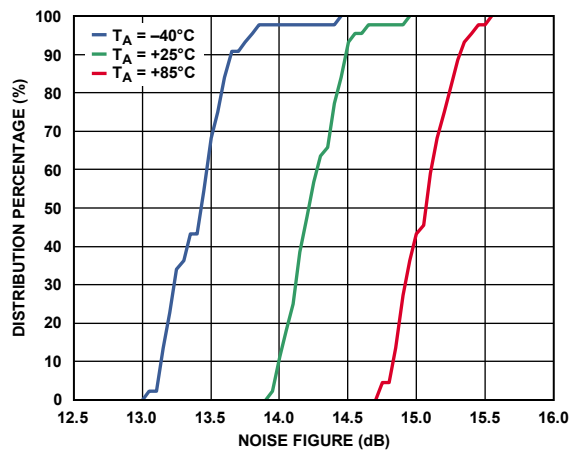


Figure 68. Noise Figure Distributions

07595-068

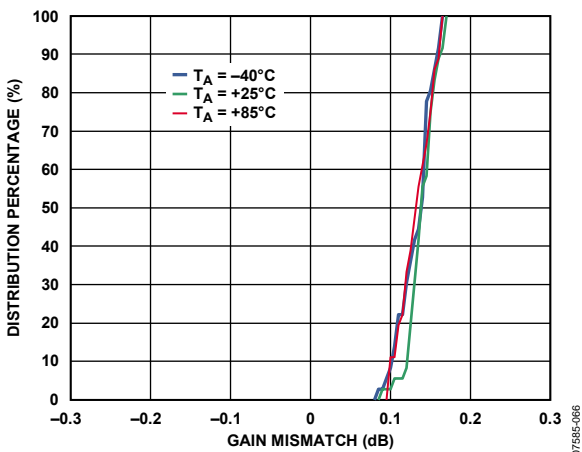


Figure 66. IQ Gain Mismatch Distributions

07595-066

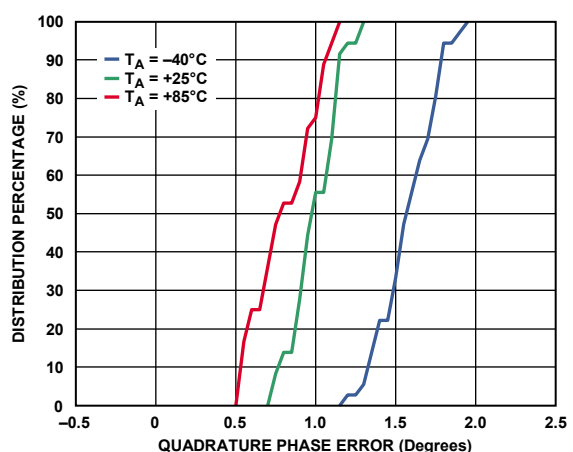


Figure 69. IQ Quadrature Phase Error Distributions

07595-069

DISTRIBUTIONS FOR  $f_{LO} = 5800$  MHz

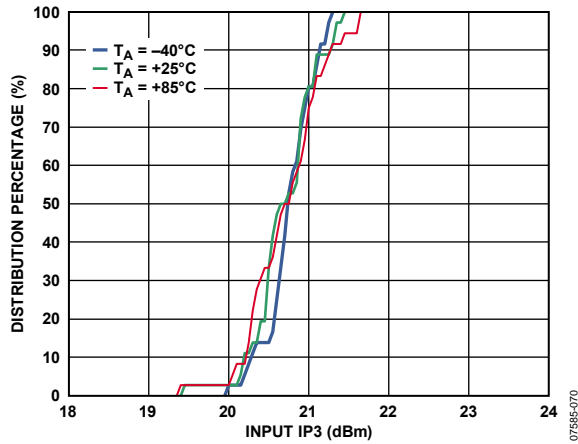


Figure 70. IIP3 Distributions

07585-070

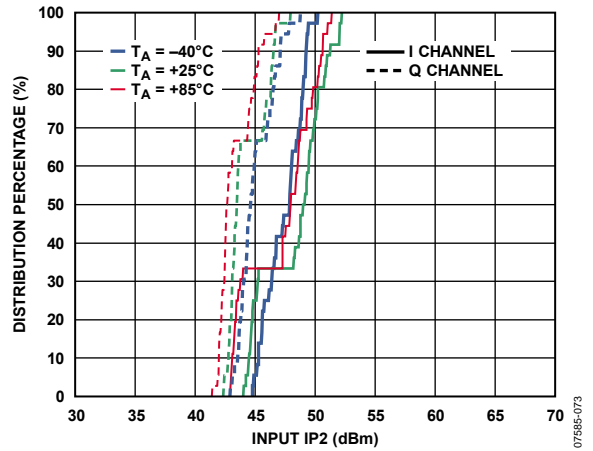


Figure 73. IIP2 Distributions for I Channel and Q Channel

07585-073

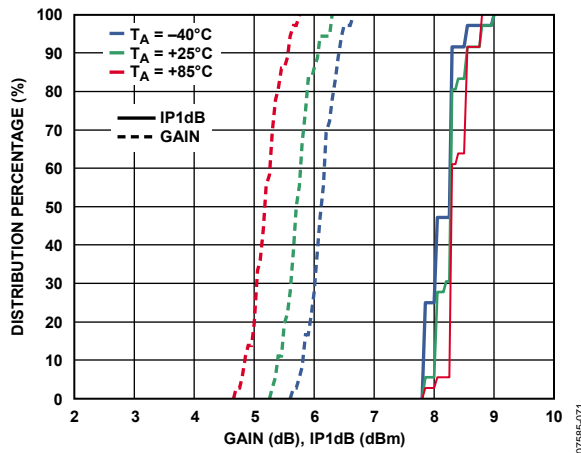


Figure 71. Gain and IP1dB Distributions

07585-071

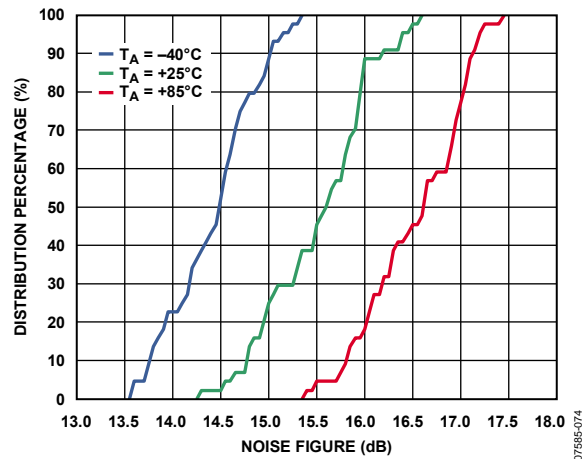


Figure 74. Noise Figure Distributions

07585-074

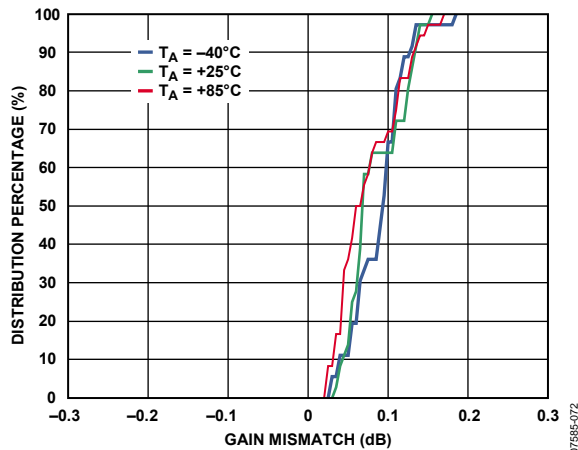


Figure 72. IQ Gain Mismatch Distributions

07585-072

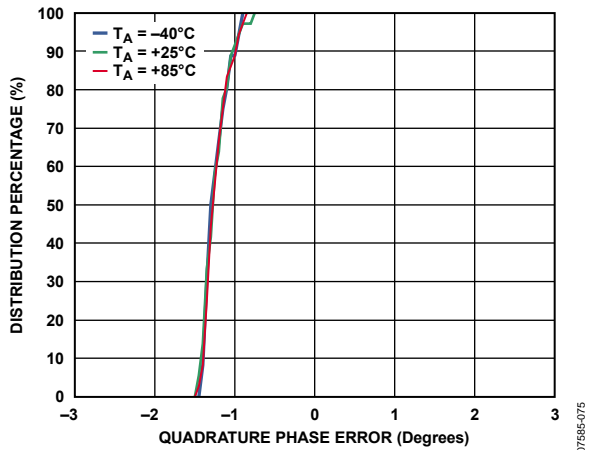


Figure 75. IQ Quadrature Phase Error Distributions

07585-075

## CIRCUIT DESCRIPTION

The ADL5380 can be divided into five sections: the local oscillator (LO) interface, the RF voltage-to-current (V-to-I) converter, the mixers, the differential emitter follower outputs, and the bias circuit. A detailed block diagram of the device is shown in Figure 76.

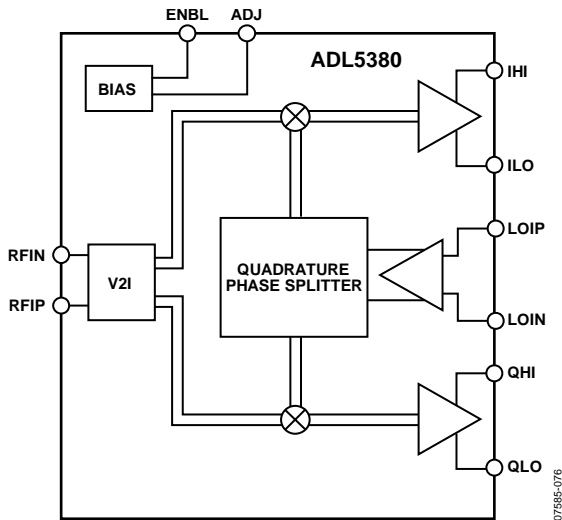


Figure 76. Block Diagram

The LO interface generates two LO signals at 90° of phase difference to drive two mixers in quadrature. RF signals are converted into currents by the V-to-I converters that feed into the two mixers. The differential I and Q outputs of the mixers are buffered via emitter followers. Reference currents to each section are generated by the bias circuit. A detailed description of each section follows.

### LO INTERFACE

The LO interface consists of a polyphase quadrature splitter followed by a limiting amplifier. The LO input impedance is set by the polyphase, which splits the LO signal into two differential signals in quadrature. The LO input impedance is nominally 50 Ω. Each quadrature LO signal then passes through a limiting amplifier that provides the mixer with a limited drive signal. For optimal performance, the LO inputs must be driven differentially.

### V-TO-I CONVERTER

The differential RF input signal is applied to a V-to-I converter that converts the differential input voltage to output currents. The V-to-I converter provides a differential 50 Ω input impedance. The V-to-I bias current can be adjusted up or down using the ADJ pin (Pin 19). Adjusting the current up improves IIP3 and IP1dB but degrades SSB NF. Adjusting the current down improves SSB NF but degrades IIP3 and IP1dB. The current adjustment can be made by connecting a resistor from the ADJ pin (Pin 19) to  $V_S$  to increase the bias current or to ground to decrease the bias current. Table 4 approximately dictates the relationship between the resistor used ( $R_{ADJ}$ ), the resulting ADJ pin voltage, and the resulting baseband common-mode output voltage.

Table 4. ADJ Pin Resistor Values and Approximate ADJ Pin Voltages

$R_{ADJ}$	$\sim V_{ADJ}$ (V)	$\sim$ Baseband Common-Mode Output (V)
200 Ω to $V_S$	4.8	2.2
600 Ω to $V_S$	4.5	2.3
1.54 kΩ to $V_S$	4	2.5
3.8 kΩ to $V_S$	3.5	2.7
10 kΩ to $V_S$	3	3
Open	2.5	3.2
9 kΩ to GND	2	3.4
3.5 kΩ to GND	1.5	3.6
1.5 kΩ to GND	1	3.8

### MIXERS

The ADL5380 has two double-balanced mixers: one for the in-phase channel (I channel) and one for the quadrature channel (Q channel). These mixers are based on the Gilbert cell design of four cross-connected transistors. The output currents from the two mixers are summed together in the resistive loads that then feed into the subsequent emitter follower buffers.

### EMITTER FOLLOWER BUFFERS

The output emitter followers drive the differential I and Q signals off chip. The output impedance is set by on-chip 25 Ω series resistors that yield a 50 Ω differential output impedance for each baseband port. The fixed output impedance forms a voltage divider with the load impedance that reduces the effective gain. For example, a 500 Ω differential load has 1 dB lower effective gain than a high (10 kΩ) differential load impedance.

### BIAS CIRCUIT

A band gap reference circuit generates the reference currents used by different sections. The bias circuit can be enabled and partially disabled using ENBL (Pin 7). If ENBL is grounded or left open, the part is fully enabled. Pulling ENBL high shuts off certain sections of the bias circuitry, reducing the standing power to about half of its fully enabled consumption and disabling the outputs.

# APPLICATIONS INFORMATION

## BASIC CONNECTIONS

Figure 77 shows the basic connections schematic for the ADL5380.

## POWER SUPPLY

The nominal voltage supply for the ADL5380 is 5 V and is applied to the VCC1, VCC2, and VCC3 pins. Connect ground to the GND1, GND2, GND3, and GND4 pins. Solder the exposed paddle on the underside of the package to a low thermal and

electrical impedance ground plane. If the ground plane spans multiple layers on the circuit board, these layers should be stitched together with nine vias under the exposed paddle. The AN-772 Application Note discusses the thermal and electrical grounding of the LFCSP in detail. Decouple each of the supply pins using two capacitors; recommended capacitor values are 100 pF and 0.1  $\mu$ F.

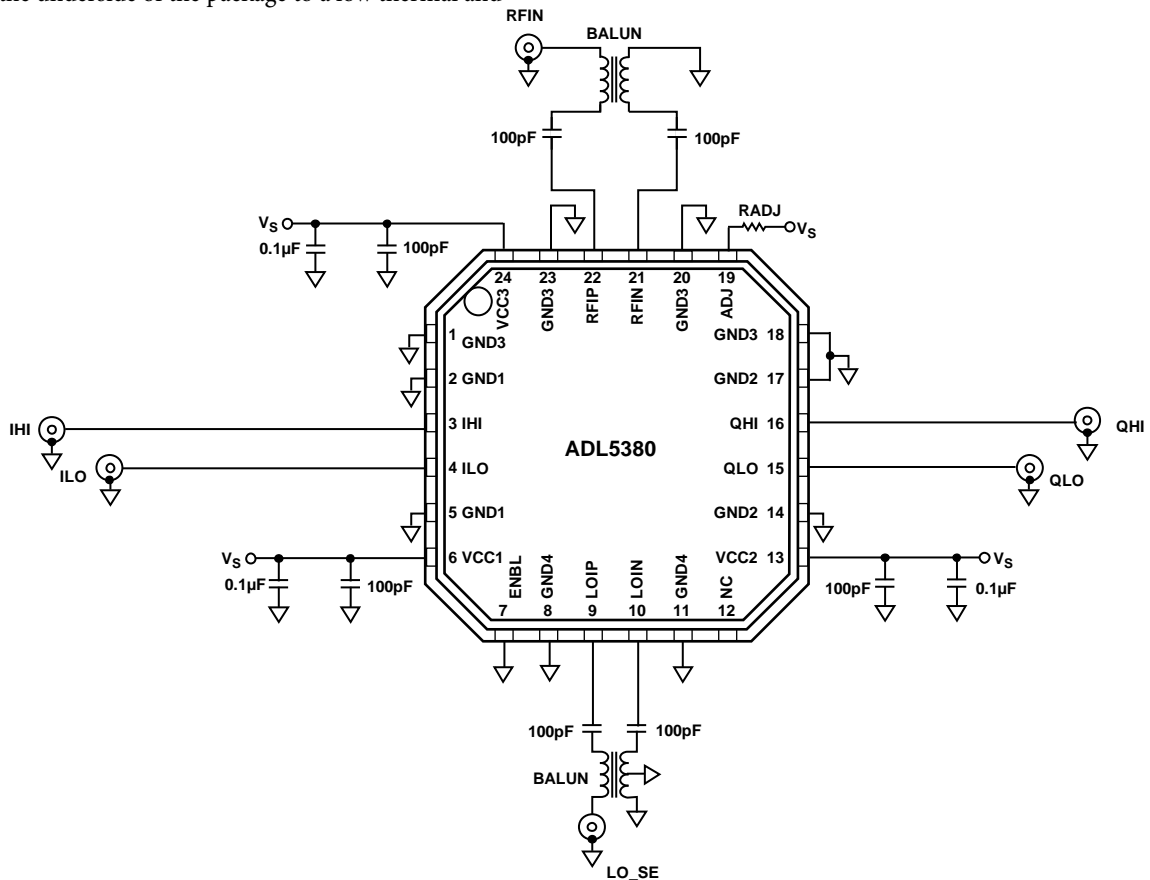


Figure 77. Basic Connections Schematic

07865-078

**LOCAL OSCILLATOR AND RF INPUTS**

The RF and LO inputs have a differential input impedance of approximately 50 Ω as shown in Figure 78. Figure 79 shows the return loss. For optimum performance, both the LO and RF ports should be ac-coupled and driven differentially through a balun as shown in Figure 80 and Figure 81. The user has many different types of balun to choose from and from a variety of manufacturers. For the data presented in this data sheet all measurements were gathered with the baluns listed below. For applications that are band specific, the recommended baluns are:

- Up to 3 GHz is the Mini-Circuits TC1-1-13.
- From 3 GHz to 4 GHz is the Johanson Technology 3600BL14M050.
- From 4.9 GHz to 6 GHz is the Johanson Technology 5400BL15B050.

For wideband applications covering the entire 400 MHz to 6 GHz range of the ADL5380, the recommended balun is the TCM1-63AX+ from Mini-Circuits. This wide and maximally flat balun allows coverage of the entire frequency range with one component.

The recommended drive level for the LO port is between -6 dBm and +6 dBm.

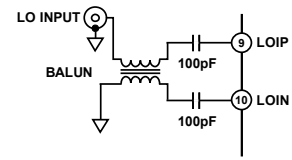


Figure 80. Differential LO Drive

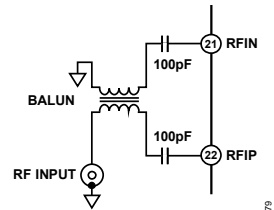


Figure 81. RF Input

Alternatively, if the single-ended drive of both the LO and RF ports is the desired mode of operation, degradations in IIP2 will be observed because of the lack of common mode rejection. The degradation in IIP2 is more prevalent at high frequencies, specifically frequencies greater than 1600 MHz. At low frequencies, the ADL5380 has inherent common mode rejection offering superior IIP2 performance in the 70 dBm range. As shown in Figure 82 and Figure 83, in single-ended mode, the largest performance impact is seen in IIP2 while minimal performance degradation is observed in IIP3.

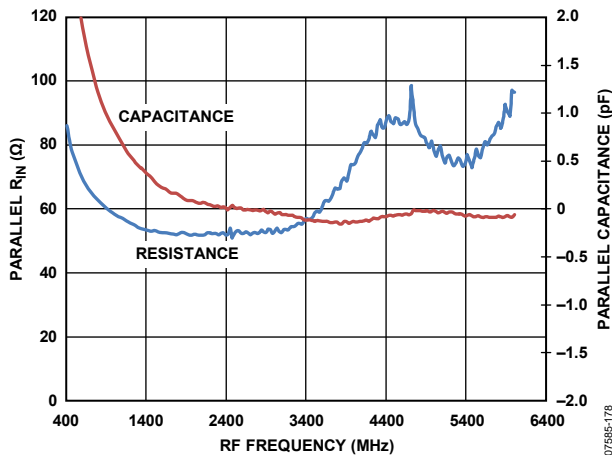


Figure 78. Differential Input Impedance of the RF Port

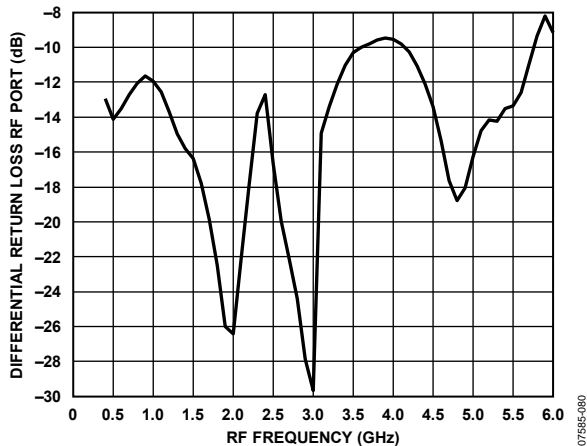


Figure 79. Differential RF Port Return Loss

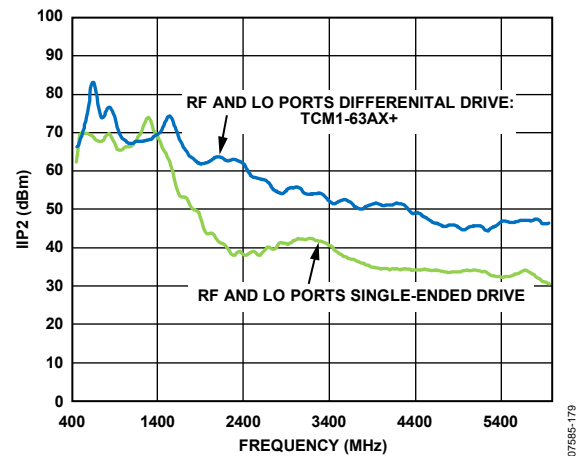


Figure 82. IIP2 vs. Frequency Comparison for Single-Ended and Differential Drive of the RF and LO Ports



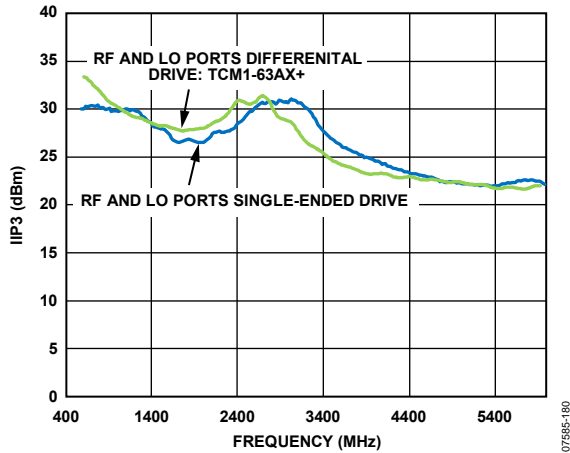


Figure 83. IIP3 vs. Frequency Comparison for Single-Ended and Differential Drive of the RF and LO Ports

To configure the **ADL5380** for single-ended drive, terminate the unused input with a 100 pF capacitor to GND while driving the alternative input. The single-ended input impedance is 25 Ω or half the differential impedance. As a result of this, ensure that there is proper impedance matching when interfacing with the **ADL5380** in single-ended mode for maximum transfer of power. Figure 84, shows an example single ended configuration when using a signal source with a 50 Ω source impedance.

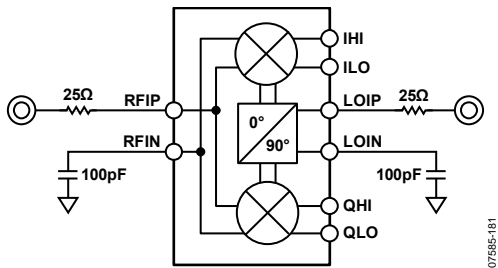


Figure 84. Single-Ended Configuration

**BASEBAND OUTPUTS**

The baseband outputs QHI, QLO, IHI, and ILO are fixed impedance ports. Each baseband pair has a 50 Ω differential output impedance. The outputs can be presented with differential loads as low as 200 Ω (with some degradation in gain) or high impedance differential loads (500 Ω or greater impedance yields the same excellent linearity) that is typical of an ADC. The TCM9-1 9:1 balun converts the differential IF output to a single-ended output. When loaded with 50 Ω, this balun presents a 450 Ω load to the device. The typical maximum linear voltage swing for these outputs is 2 V p-p differential. The output 3 dB bandwidth is 390 MHz. Figure 85 shows the baseband output configuration.

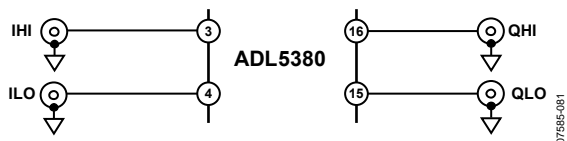


Figure 85. Baseband Output Configuration

**ERROR VECTOR MAGNITUDE (EVM) PERFORMANCE**

EVM is a measure used to quantify the performance of a digital radio transmitter or receiver. A signal received by a receiver has all constellation points at their ideal locations; however, various imperfections in the implementation (such as magnitude imbalance, noise floor, and phase imbalance) cause the actual constellation points to deviate from their ideal locations.

In general, a demodulator exhibits three distinct EVM limitations vs. received input signal power. At strong signal levels, the distortion components falling in-band due to nonlinearities in the device cause strong degradation to EVM as signal levels increase. At medium signal levels, where the demodulator behaves in a linear manner and the signal is well above any notable noise contributions, the EVM has a tendency to reach an optimum level determined dominantly by the quadrature accuracy of the demodulator and the precision of the test equipment. As signal levels decrease, such that noise is a major contribution, the EVM performance vs. the signal level exhibits a decibel-for-decibel degradation with decreasing signal level. At lower signal levels, where noise proves to be the dominant limitation, the decibel EVM proves to be directly proportional to the SNR.

The **ADL5380** shows excellent EVM performance for various modulation schemes. Figure 86 shows the EVM performance of the **ADL5380** with a 16 QAM, 200 kHz low IF.

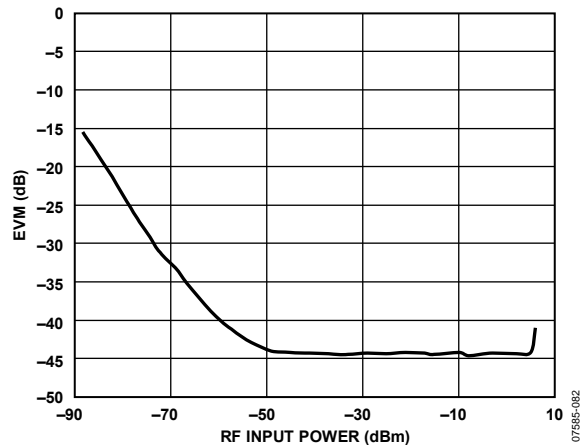


Figure 86. EVM, RF = 900 MHz, IF = 200 kHz vs. RF Input Power for a 16 QAM 160ksym/s Signal

Figure 87 shows the zero-IF EVM performance of a 10 MHz IEEE 802.16e WiMAX signal through the ADL5380. The differential dc offsets on the ADL5380 are in the order of a few millivolts. However, ac coupling the baseband outputs with 10  $\mu$ F capacitors eliminates dc offsets and enhances EVM performance. With a 10 MHz BW signal, 10  $\mu$ F ac coupling capacitors with the 500  $\Omega$  differential load results in a high-pass corner frequency of  $\sim$ 64 Hz, which absorbs an insignificant amount of modulated signal energy from the baseband signal. By using ac coupling capacitors at the baseband outputs, the dc offset effects, which can limit dynamic range at low input power levels, can be eliminated.

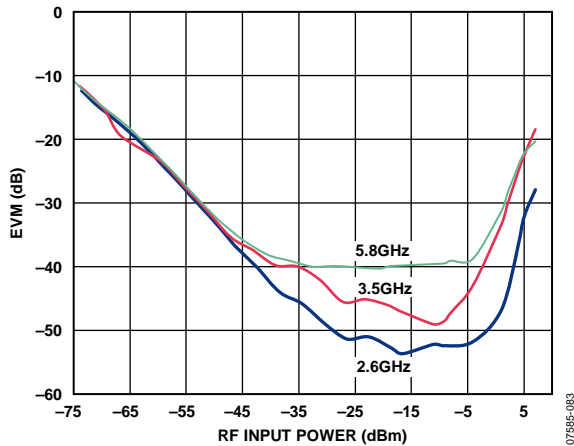


Figure 87. EVM, RF = 2.6 GHz, RF = 3.5 GHz, and RF = 5.8 GHz, IF = 0 Hz vs. RF Input Power for a 16 QAM 10 MHz Bandwidth Mobile WiMAX Signal (AC-Coupled Baseband Outputs)

Figure 88 exhibits multiple W-CDMA low-IF EVM performance curves over a wide RF input power range into the ADL5380. In the case of zero-IF, the noise contribution by the vector signal analyzer becomes predominant at lower power levels, making it difficult to measure SNR accurately.

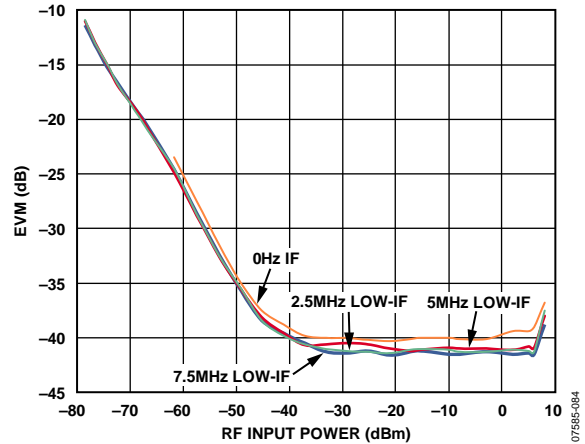


Figure 88. EVM, RF = 1900 MHz, IF = 0 Hz, IF = 2.5 MHz, IF = 5 MHz, and IF = 7.5 MHz vs. RF Input Power for a W-CDMA Signal (AC-Coupled Baseband Outputs)

**LOW IF IMAGE REJECTION**

The image rejection ratio is the ratio of the intermediate frequency (IF) signal level produced by the desired input frequency to that produced by the image frequency. The image rejection ratio is expressed in decibels. Appropriate image rejection is critical because the image power can be much higher than that of the desired signal, thereby plaguing the down-conversion process. Figure 89 illustrates the image problem. If the upper sideband (lower sideband) is the desired band, a 90° shift to the Q channel (I channel) cancels the image at the lower sideband (upper sideband). Phase and gain balance between I and Q channels are critical for high levels of image rejection.

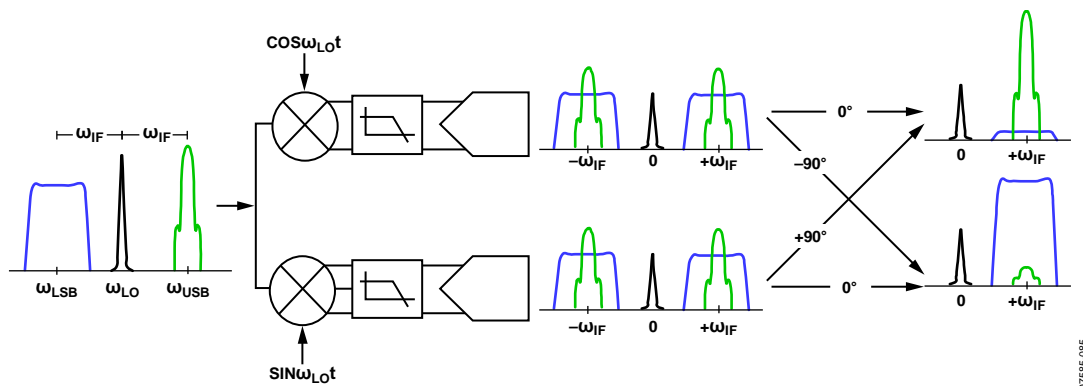


Figure 89. Illustration of the Image Problem

Figure 90 and Figure 91 show the excellent image rejection capabilities of the ADL5380 for low IF applications, such as W-CDMA. The ADL5380 exhibits image rejection greater than 45 dB over a broad frequency range.

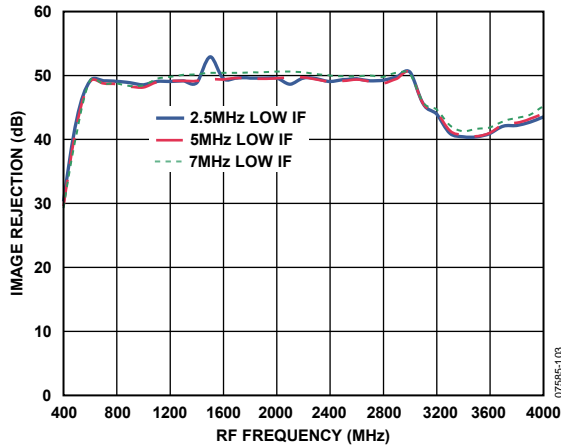


Figure 90. Low Band and Midband Image Rejection vs. RF Frequency for a W-CDMA Signal, IF = 2.5 MHz, 5 MHz, and 7.5 MHz

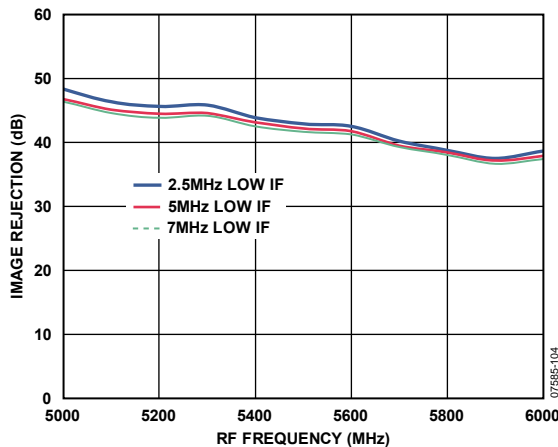


Figure 91. High Band Image Rejection vs. RF Frequency for a W-CDMA Signal, IF = 2.5 MHz, 5 MHz, and 7.5 MHz

### EXAMPLE BASEBAND INTERFACE

In most direct-conversion receiver designs, it is desirable to select a wanted carrier within a specified band. The desired channel can be demodulated by tuning the LO to the appropriate carrier frequency. If the desired RF band contains multiple carriers of interest, the adjacent carriers are also down converted to a lower IF frequency. These adjacent carriers can be problematic if they are large relative to the wanted carrier because they can overdrive the baseband signal detection circuitry. As a result, it is often necessary to insert a filter to provide sufficient rejection of the adjacent carriers.

It is necessary to consider the overall source and load impedance presented by the ADL5380 and ADC input when designing the filter network. The differential baseband output impedance of the ADL5380 is 50 Ω. The ADL5380 is designed to drive a high impedance ADC input. It may be desirable to terminate the ADC input down to lower impedance by using a terminating resistor, such as 500 Ω. The terminating resistor helps to better define the input impedance at the ADC input at the cost of a slightly reduced gain (see the Circuit Description section for details on the emitter-follower output loading effects).

The order and type of filter network depends on the desired high frequency rejection required, pass-band ripple, and group delay. Filter design tables provide outlines for various filter types and orders, illustrating the normalized inductor and capacitor values for a 1 Hz cutoff frequency and 1 Ω load. After scaling the normalized prototype element values by the actual desired cut-off frequency and load impedance, the series reactance elements are halved to realize the final balanced filter network component values.

As an example, a second-order Butterworth, low-pass filter design is shown in Figure 92 where the differential load impedance is 500 Ω and the source impedance of the ADL5380 is 50 Ω. The normalized series inductor value for the 10-to-1, load-to-source impedance ratio is 0.074 H, and the normalized shunt capacitor is 14.814 F. For a 10.9 MHz cutoff frequency, the single-ended equivalent circuit consists of a 0.54 μH series inductor followed by a 433 pF shunt capacitor.

The balanced configuration is realized as the 0.54 μH inductor is split in half to realize the network shown in Figure 92.

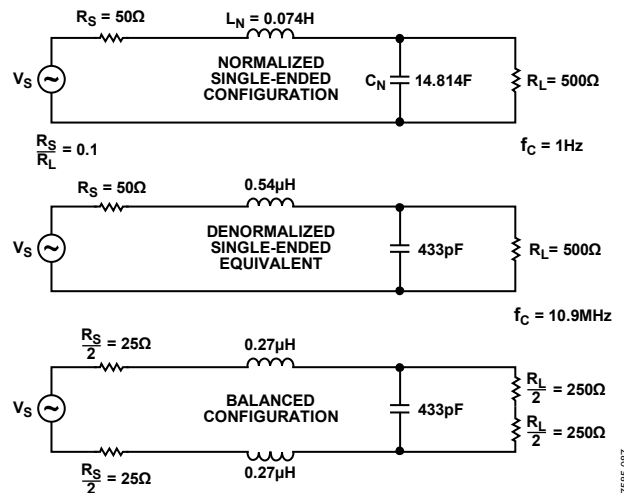


Figure 92. Second-Order Butterworth, Low-Pass Filter Design Example

A complete design example is shown in Figure 95. A sixth-order Butterworth differential filter having a 1.9 MHz corner frequency interfaces the output of the ADL5380 to that of an ADC input. The 500 Ω load resistor defines the input impedance of the ADC. The filter adheres to typical direct conversion W-CDMA applications where, 1.92 MHz away from the carrier IF frequency, 1 dB of rejection is desired, and, 2.7 MHz away from the carrier IF frequency, 10 dB of rejection is desired.

Figure 93 and Figure 94 show the measured frequency response and group delay of the filter.

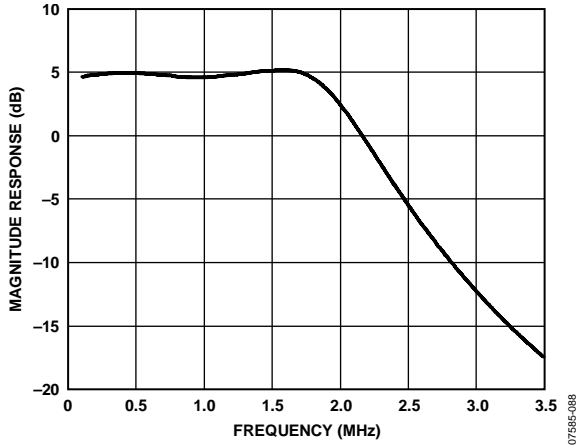


Figure 93. Sixth-Order Baseband Filter Response

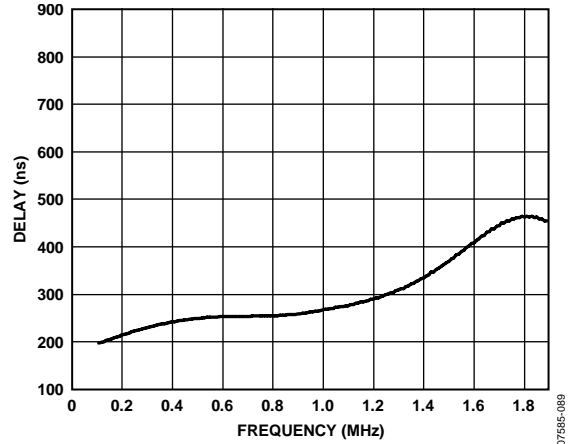


Figure 94. Sixth-Order Baseband Filter Group Delay

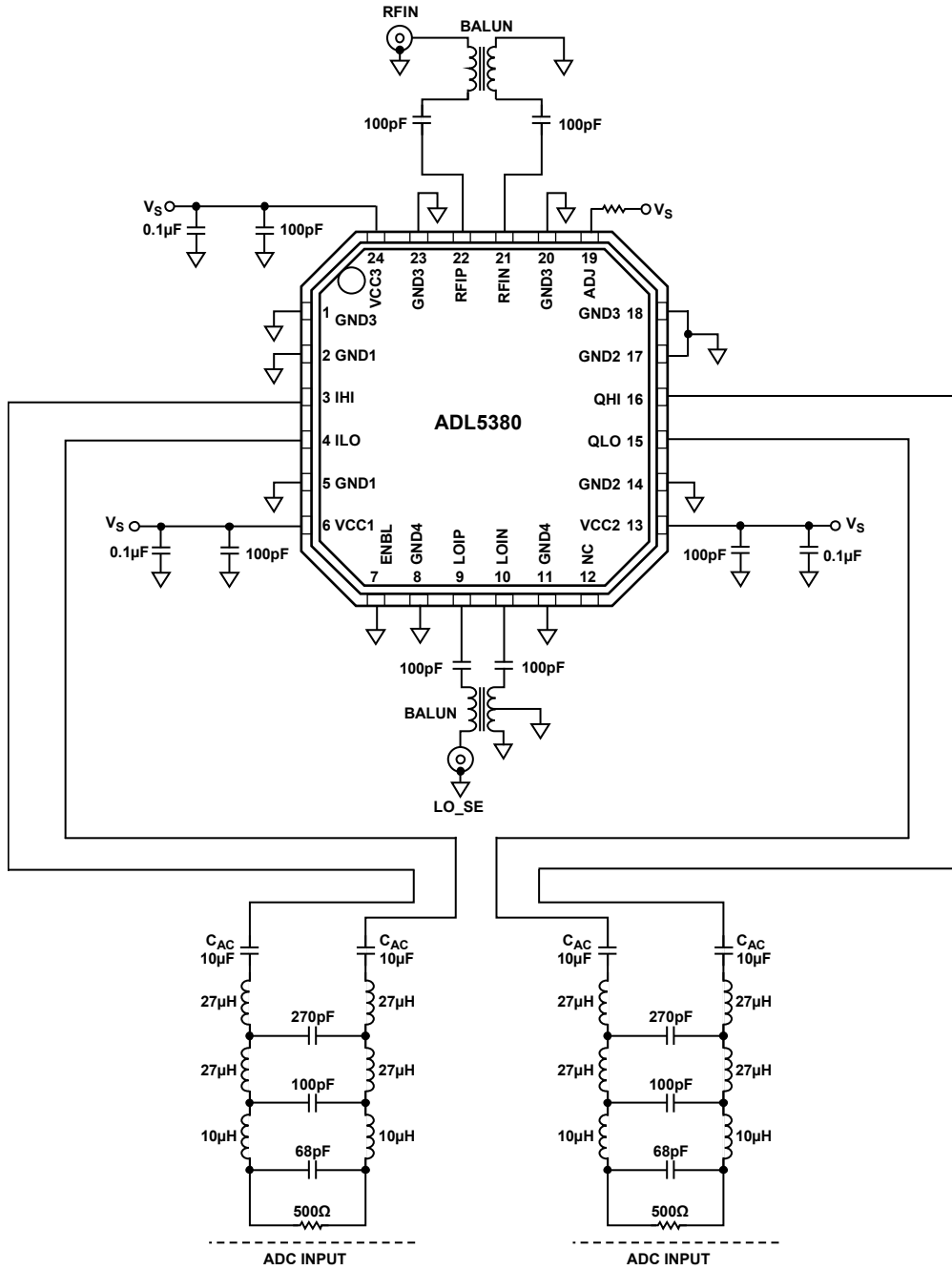


Figure 95. Sixth-Order Low-Pass Butterworth, Baseband Filter Schematic

07595-090

As the load impedance of the filter increases, the filter design becomes more challenging in terms of meeting the required rejection and pass band specifications. In the previous W-CDMA example, the 500 Ω load impedance resulted in the design of a sixth-order filter that has relatively large inductor values and small capacitor values. If the load impedance is 200 Ω, the filter design becomes much more manageable. Figure 96 shows a fourth-order filter designed for a 10 MHz wide LTE signal. As shown in Figure 96, the resultant inductor and capacitor values become much more practical with a 200 Ω load.

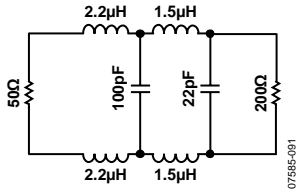


Figure 96. Fourth-Order Low-Pass LTE Filter Schematic

Figure 97 and Figure 98 illustrate the magnitude response and group delay response of the fourth-order filter, respectively.

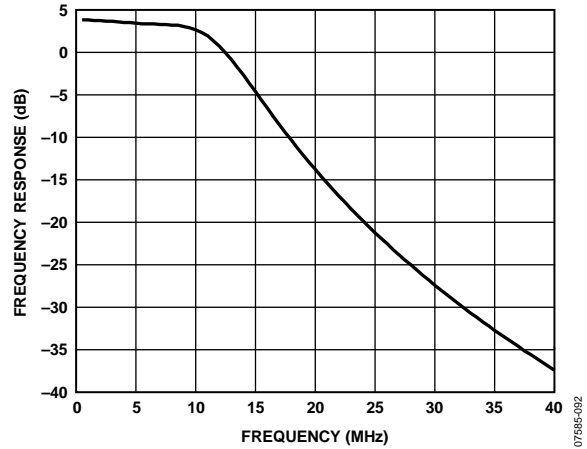


Figure 97. Fourth-Order Low-Pass LTE Filter Magnitude Response

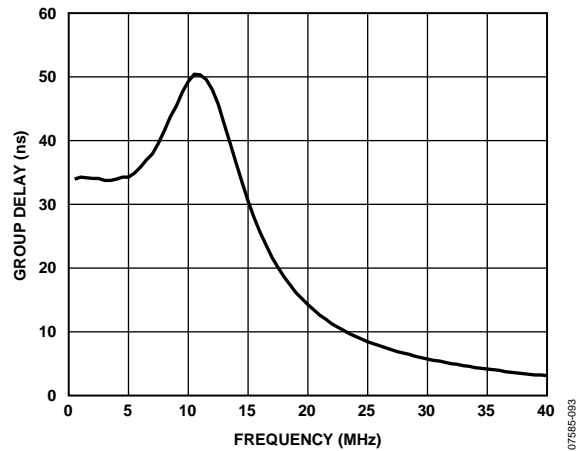


Figure 98. Fourth-Order Low-Pass LTE Filter Group Delay Response

## CHARACTERIZATION SETUPS

Figure 99 to Figure 101 show the general characterization bench setups used extensively for the ADL5380. The setup shown in Figure 101 was used to do the bulk of the testing and used sinusoidal signals on both the LO and RF inputs. An automated Agilent VEE program was used to control the equipment over the IEEE bus. This setup was used to measure gain, IP1dB, IIP2, IIP3, I/Q gain match, and quadrature error. The ADL5380 characterization board had a 9-to-1 impedance transformer on each of the differential baseband ports to do the differential-to-single-ended conversion, which presented a 450  $\Omega$  differential load to each baseband port, when interfaced with 50  $\Omega$  test equipment.

For all measurements of the ADL5380, the loss of the RF input balun was de-embedded. Due to the wideband nature of the ADL5380, three different board configurations had to be used to characterize the product. For low band characterization (400 MHz to 3 GHz), the Mini-Circuits TC1-1-13 balun was used on the RF and LO inputs to create differential signals at the device pins. For midband characterization (3 GHz to 4 GHz), the Johanson Technology 3600BL14M050T was used, and for high band characterization (5 GHz to 6 GHz), the Johanson Technology 5400BL15B050E balun was used.

The two setups shown in Figure 99 and Figure 100 were used for making NF measurements. Figure 99 shows the setup for measuring NF with no blocker signal applied while Figure 100 was used to measure NF in the presence of a blocker. For both setups, the noise was measured at a baseband frequency of 10 MHz. For the case where a blocker was applied, the output blocker was at a 15 MHz baseband frequency. Note that great care must be taken when measuring NF in the presence of a blocker. The RF blocker generator must be filtered to prevent its noise (which increases with increasing generator output power) from swamping the noise contribution of the ADL5380. At least 30 dB of attenuation at the RF and image frequencies is desired. For example, assume a 915 MHz signal applied to the LO inputs of the ADL5380. To obtain a 15 MHz output blocker signal, the RF blocker generator is set to 930 MHz and the filters tuned such that there is at least 30 dB of attenuation from the generator at both the desired RF frequency (925 MHz) and the image RF frequency (905 MHz). Finally, the blocker must be removed from the output (by the 10 MHz low-pass filter) to prevent the blocker from swamping the analyzer.

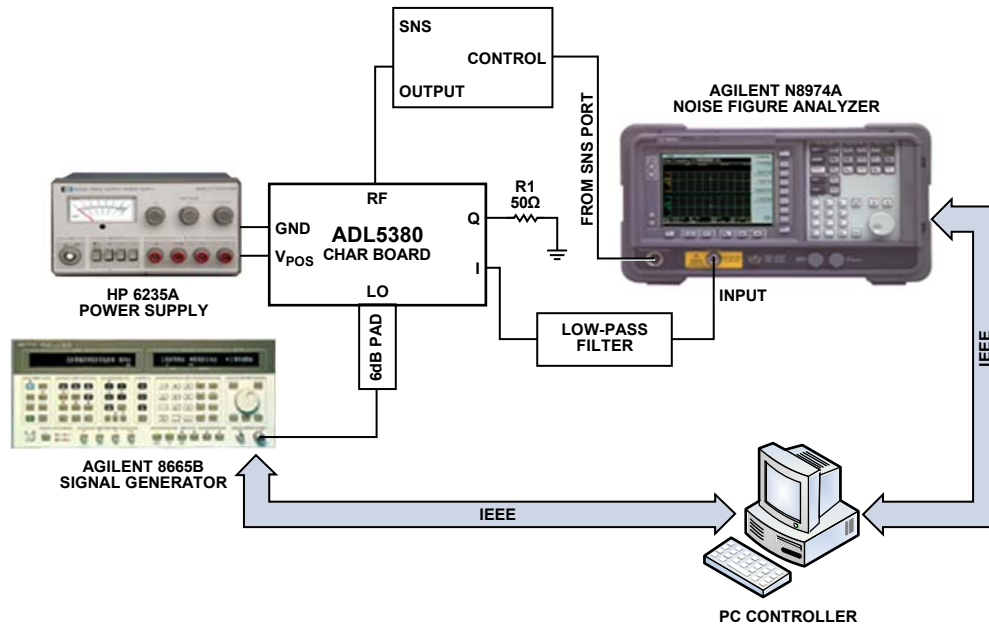


Figure 99. General Noise Figure Measurement Setup

07585-095

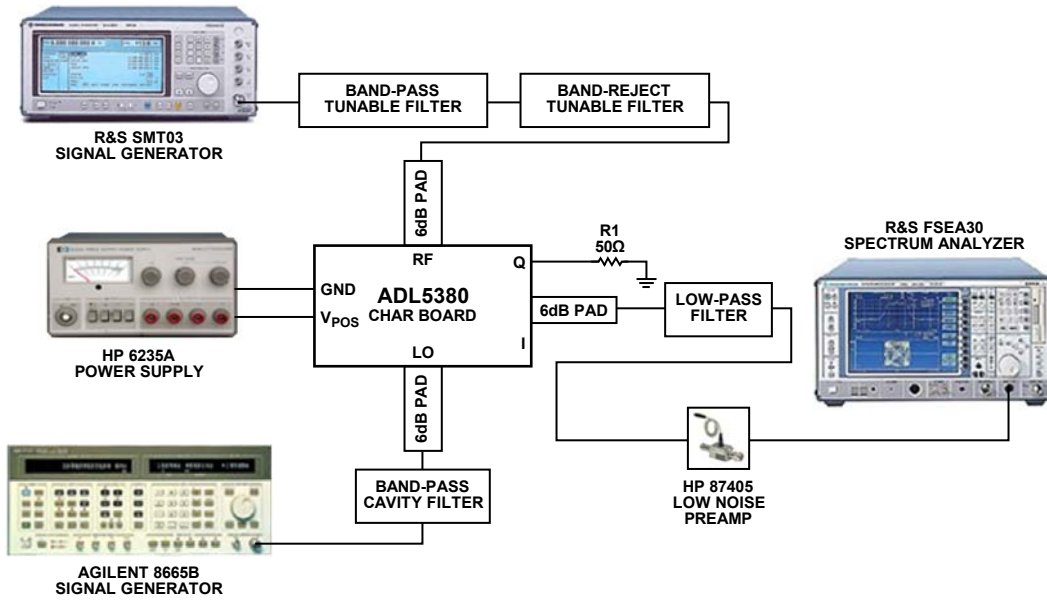


Figure 100. Measurement Setup for Noise Figure in the Presence of a Blocker

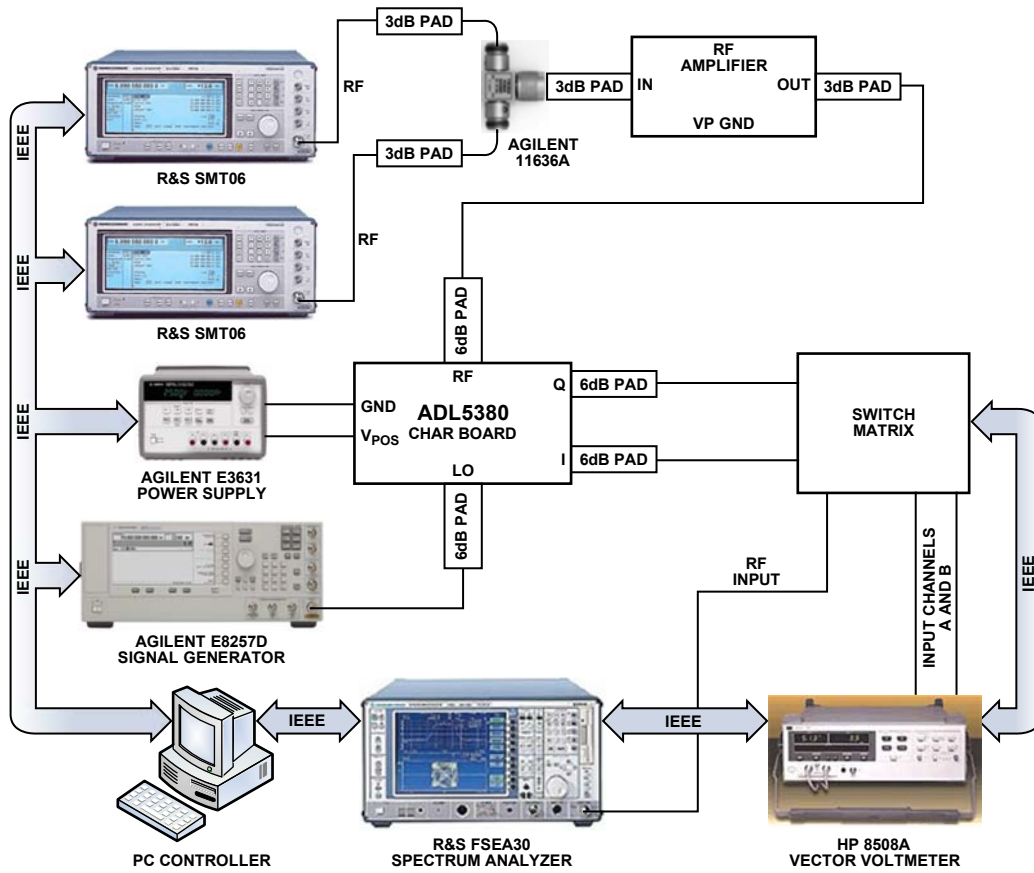


Figure 101. General Characterization Setup



### EVALUATION BOARD

The **ADL5380** evaluation board is available. The evaluation board is populated with the wide band TCM1-63AX+ transformer from Mini-Circuits. This transformer covers the entire frequency range of the **ADL5380** from 400 MHz to 6 GHz.

The board can be used for single-ended or differential baseband analysis. The default configuration of the board is for single-ended baseband analysis.

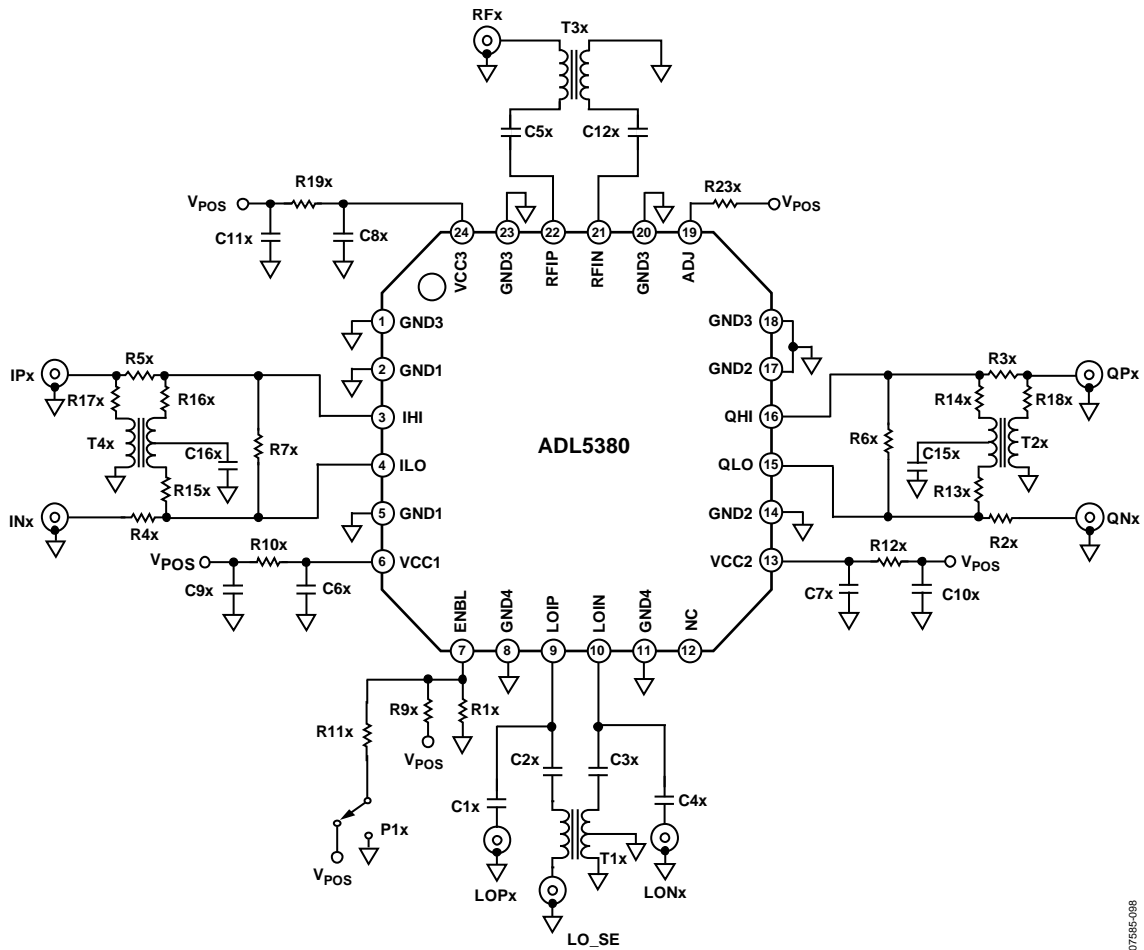


Figure 102. Evaluation Board Schematic

07585-098

Table 5. Evaluation Board Configuration Options

Component	Description	Default Condition
VPOSx, GNDx	Power Supply and Ground Vector Pins.	Not applicable
R10x, R12x, R19x	Power Supply Decoupling. Shorts or power supply decoupling resistors.	R10x, R12x, R19x = 0 Ω (0603)
C6x to C11x	The capacitors provide the required dc coupling up to 6 GHz.	C6x, C7x, C8x = 100 pF (0402), C9x, C10x, C11x = 0.1 μF (0603)
P1x, R11x, R9x, R1x	Device Enable. When connected to V <sub>s</sub> , the device is active.	P1x, R9x = DNI, R1x = DNI, R11x = 0 Ω
R23x	Adjust Pin. The resistor value here sets the bias voltage at this pin and optimizes third-order distortion.	R23x = 1.5 kΩ (0603)
C1x to C5x, C12x	AC Coupling Capacitors. These capacitors provide the required ac coupling from 400 MHz to 4 GHz.	C1x, C4x = DNI, C2x, C3x, C5x, C12x = 100 pF (0402)
R2x to R7x, R13x to R18x	Single-Ended Baseband Output Path. This is the default configuration of the evaluation board. R13x to R18x are populated for appropriate balun interface. R2x to R5x are not populated. Baseband outputs are taken from QHI and IHI. The user can reconfigure the board to use full differential baseband outputs. R2x to R5x provide a means to bypass the 9:1 TCM9-1 transformer to allow for differential baseband outputs. Access the differential baseband signals by populating R2x to R5x with 0 Ω and not populating R13x to R18x. This way the transformer does not need to be removed. The baseband outputs are taken from the SMAs of QHI, QLO, IHI, and ILO. R6x and R7x are provisions for applying a specific differential load across the baseband outputs	R2x to R7x = open, R13x to R18x = 0 Ω (0402)
T2x, T4x	IF Output Interface. TCM9-1 converts a differential high impedance IF output to a single-ended output. When loaded with 50 Ω, this balun presents a 450 Ω load to the device. The center tap can be decoupled through a capacitor to ground.	T2x, T4x = TCM9-1, 9:1 (Mini-Circuits)
C15x, C16x	Decoupling Capacitors. C15x and C16x are the decoupling capacitors used to reject noise on the center tap of the TCM9-1.	C15x, C16x = 0.1 μF (0402)
T1x	LO Input Interface. A 1:1 RF balun that converts the single-ended RF input to differential signal is used.	TCM1-63AX+
T3x	RF Input Interface. A 1:1 RF balun that converts the single-ended RF input to differential signal is used.	TCM1-63AX+

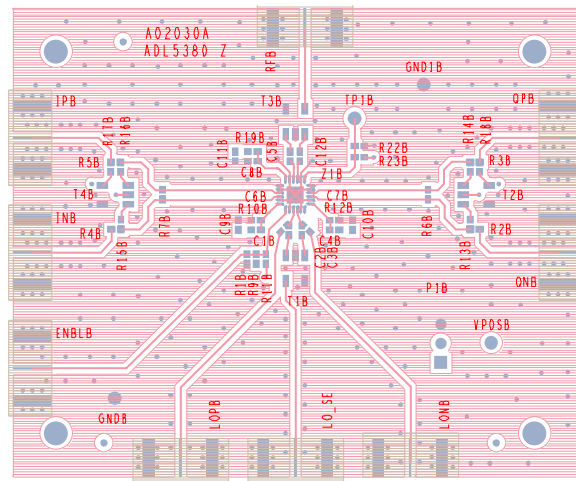


Figure 103. Evaluation Board Top Layer

### THERMAL GROUNDING AND EVALUATION BOARD LAYOUT

The package for the [ADL5380](#) features an exposed paddle on the underside that should be well soldered to a low thermal and electrical impedance ground plane. This paddle is typically soldered to an exposed opening in the solder mask on the evaluation board. Figure 104 illustrates the dimensions used in the layout of the [ADL5380](#) footprint on the [ADL5380](#) evaluation board (1 mil = 0.0254 mm).

Notice the use of nine via holes on the exposed paddle. These ground vias should be connected to all other ground layers on the evaluation board to maximize heat dissipation from the device package.

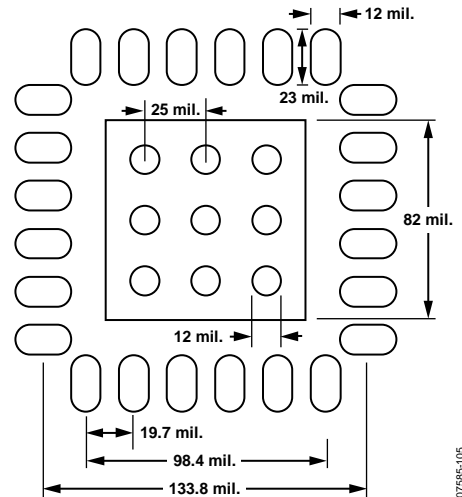
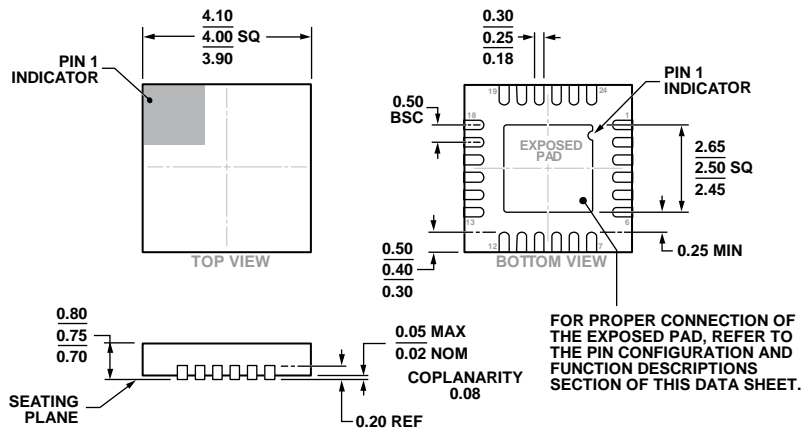


Figure 104. Dimensions for Evaluation Board Layout for the [ADL5380](#) Package

Under these conditions, the thermal impedance of the [ADL5380](#) was measured to be approximately 30°C/W in still air.

OUTLINE DIMENSIONS



COMPLIANT TO JEDEC STANDARDS MO-220-WGGD.

Figure 105. 24-Lead Lead Frame Chip Scale Package [LFCSP\_WQ]  
 4 mm × 4 mm Body, Very Very Thin Quad  
 (CP-24-7)  
 Dimensions shown in millimeters

03-11-2013-A

ORDERING GUIDE

Model <sup>1</sup>	Temperature Range	Package Description	Package Option	Ordering Quantity
ADL5380ACPZ-R7	-40°C to +85°C	24-Lead LFCSP_WQ	CP-24-7	1,500, 7" Tape and Reel
ADL5380ACPZ-WP	-40°C to +85°C	24-Lead LFCSP_WQ	CP-24-7	64, Waffle Pack
ADL5380-EVALZ				1

<sup>1</sup> Z = RoHS Compliant Part.